

**Bachelor Project**



**Czech  
Technical  
University  
in Prague**

**F3**

**Faculty of Electrical Engineering  
Department of Measurement**

## **Modular fluxgate magnetometer with digital output**

**Martin Pešek**

**Supervisor: Ing. Vojtěch Petrucha, Ph.D.  
Field of study: Cybernetics and Robotics  
Subfield: Systems and control  
May 2018**



## I. OSOBNÍ A STUDIJNÍ ÚDAJE

Příjmení: **Pešek** Jméno: **Martin** Osobní číslo: **456926**  
Fakulta/ústav: **Fakulta elektrotechnická**  
Zadávající katedra/ústav: **Katedra řídicí techniky**  
Studijní program: **Kybernetika a robotika**  
Studijní obor: **Systemy a řízení**

## II. ÚDAJE K BAKALÁŘSKÉ PRÁCI

Název bakalářské práce:

**Modulový fluxgate magnetometr s digitálním výstupem**

Název bakalářské práce anglicky:

**Modular Fluxgate Magnetometer with Digital Output**

Pokyny pro vypracování:

1. Navrhněte a realizujte kompletní elektroniku pro fluxgate magnetometr s digitálním výstupem. Jako řídicí mikrokontrolér zvolte vhodný typ z řady STM32 a vytvořte a otestujte potřebný firmware tak, aby  
a) magnetometr umožňoval zobrazení naměřených hodnot na displeji, odesílání přes sběrnici RS232 a ukládání na microSD kartu;  
b) jednotlivé parametry přístroje byly konfigurovatelné z menu na displeji nebo přes PC (rozhraní RS232 nebo USB).
2. Sestavený magnetometr zkalibrujte a porovnejte s dostupnými zařízeními na trhu.

Seznam doporučené literatury:

- [1] Rob Toulson, Tim Wilmshurst: Fast and Effective Embedded Systems Design, Newnes 2017
- [2] Pavel Ripka: Magnetic Sensors and Magnetometers, Artech House Remote Sensing Library
- [3] Mark I. Montrose: EMC and the Printed Circuit Board: Design, Theory, and Layout Made Simple, IEEE 1999
- [4] Vít Záhlava: Návrh a konstrukce DPS, Ben 2010

Jméno a pracoviště vedoucí(ho) bakalářské práce:

**Ing. Vojtěch Petrucha, Ph.D., 13138**

Jméno a pracoviště druhé(ho) vedoucí(ho) nebo konzultanta(ky) bakalářské práce:

Datum zadání bakalářské práce: **22.01.2018**

Termín odevzdání bakalářské práce: **25.05.2018**

Platnost zadání bakalářské práce: **30.09.2019**

Ing. Vojtěch Petrucha, Ph.D.  
podpis vedoucí(ho) práce

prof. Ing. Michael Šebek, DrSc.  
podpis vedoucí(ho) ústavu/katedry

prof. Ing. Pavel Ripka, CSc.  
podpis děkana(ky)

## III. PŘEVZETÍ ZADÁNÍ

Student bere na vědomí, že je povinen vypracovat bakalářskou práci samostatně, bez cizí pomoci, s výjimkou poskytnutých konzultací. Seznam použité literatury, jiných pramenů a jmen konzultantů je třeba uvést v bakalářské práci.

\_\_\_\_\_  
Datum převzetí zadání

\_\_\_\_\_  
Podpis studenta



## Acknowledgements

I would foremost like to thank my supervisor for his pieces of advice and his patience. I also want to express gratitude towards my relatives for creating a peaceful environment suitable for work.

## Declaration

I hereby declare that I have completed this thesis individually and that I have listed all used information sources in accordance with "Metodický pokyn o držování etických principů při přípravě vysokoškolských závěrečných prací".

In Trutnov, 7 May 2018

## Abstract

Aim of this thesis was to design and realize unique highly precise fluxgate magnetometer with digital output and other optional functions, development of which is motivated by demanding requirements of potential users.

Summary of current competition's products and comparison of specifications may be found in this thesis.

There can also be seen design details (electrical circuit, printed circuit board and firmware) of our product including a comparison of theoretical results with the real ones that are an outcome of the realization, progress of which is described in this thesis.

**Keywords:** magnetometer, fluxgate, STM

**Supervisor:** Ing. Vojtěch Petrucha, Ph.D.

## Abstrakt

Záměrem této práce bylo navržení a realizace unikátního vysoce přesného fluxgate magnetometru s digitálním výstupem a dalšími volitelnými funkcemi, jehož vývoj je motivován náročnými požadavky potenciálních uživatelů.

V této práci lze nalézt přehled současných konkurenčních výrobků a porovnání specifikací.

Jsou zde uvedeny návrhové detaily (elektrický obvod, deska tištěných spojů a firmware) našeho produktu včetně porovnání očekávaných výsledků se skutečnými, které jsou výstupem realizace, jejíž postup je také součástí této práce.

**Klíčová slova:** magnetometr, fluxgate, STM

**Překlad názvu:** Modulový fluxgate magnetometr s digitálním výstupem

# Contents

|   |           |
|---|-----------|
| <b>1 Introduction and motivation</b>                          | <b>1</b>  |
| <b>2 Theoretical analysis</b>                                 | <b>3</b>  |
| 2.1 Magnetometers .....                                       | 3         |
| 2.2 Fluxgate magnetometer .....                               | 3         |
| 2.3 State of the art .....                                    | 4         |
| <b>3 Device conception</b>                                    | <b>7</b>  |
| 3.1 Electrical circuit design .....                           | 7         |
| 3.1.1 MCU .....   | 8         |
| 3.1.2 Power .....   | 9         |
| 3.1.3 Excitation .....  | 11        |
| 3.1.4 Digitization .....                                      | 12        |
| 3.1.5 Communication .....                                     | 15        |
| 3.1.6 EEPROM .....  | 18        |
| 3.1.7 Temperature sensors .....                               | 19        |
| 3.1.8 HMI .....   | 20        |
| 3.2 PCB design .....  | 22        |
| 3.2.1 General methodology .....                               | 23        |
| 3.2.2 Top layer .....   | 24        |
| 3.2.3 Ground planes layer .....                               | 25        |
| 3.2.4 Voltage planes layer .....                              | 26        |
| 3.2.5 Bottom layer .....                                      | 26        |
| <b>4 Firmware</b>   | <b>27</b> |
| 4.1 Basic concept .....                                       | 27        |
| 4.2 Start-up .....  | 28        |
| 4.3 Main program .....  | 30        |
| 4.3.1 Front-end .....   | 30        |
| 4.3.2 Back-end .....  | 32        |
| <b>5 Realization</b>  | <b>35</b> |
| 5.1 Firmware .....  | 35        |
| 5.2 Hardware .....  | 36        |
| 5.3 Tuning .....  | 37        |
| 5.4 Parameters measuring .....                                | 38        |
| 5.4.1 Noise .....   | 38        |
| 5.4.2 Calibration .....                                       | 38        |
| <b>6 Conclusion</b>   | <b>43</b> |
| <b>A Schematics drawings</b>                                  | <b>45</b> |
| <b>B Control commands for terminal<br/>over RS-232 or USB</b> | <b>53</b> |
| <b>C Bibliography</b>   | <b>55</b> |

## Figures

|   |    |  |    |
|---|----|--|----|
| 1.1 Berringer Crater, Arizona [1] . . . .   | 1  | 4.3 Flowchart of device's main program . . . . .   | 31 |
| 2.1 Block diagram of a second harmonic fluxgate magnetometer [2, p. 91] . . . . .                           | 4  | 4.4 Basic modules dependency graph generated by Graphviz . . . . .   | 33 |
| 3.1 Block scheme of our fluxgate magnetometer . . . . .   | 7  | 5.1 USB testing on our development kit . . . . .   | 35 |
| 3.2 Circuitry of crystal oscillator and battery cell . . . . .  | 8  | 5.2 Finished and working device . . . . .  | 36 |
| 3.3 Connection of programming pins . . . . .  | 9  | 5.3 Tuning of the second harmonic on the sensor output (purple) and excitation current (yellow) . . . . .                                      | 37 |
| 3.4 Protection on input of power supply . . . . .   | 10 | 5.4 Setting the phase between excitation control voltage (yellow) and switching voltage (purple) by assessing the PSD output (green) . . . . . | 37 |
| 3.5 Output of LTC3115 . . . . .   | 10 | 5.5 Noise spectral density of data sampled on Y channel with 62.5 sps sampling . . . . .   | 38 |
| 3.6 Adjustable regulator LT1763 [3] . . . . .   | 11 | 5.6 Angles defining non-orthogonality [5] . . . . .  | 39 |
| 3.7 Excitation circuit . . . . .  | 12 | 5.7 ADC conversion function for Y channel . . . . .  | 40 |
| 3.8 Input circuitry of signal processing . . . . .  | 13 | 5.8 Scalar calibration process in Průhonice . . . . .  | 40 |
| 3.9 Unity gain buffer suitable for capacitive loads . . . . .   | 14 | 5.9 Scalar calibration plots of vector magnitude and residuals . . . . .   | 41 |
| 3.10 Reference voltage circuitry . . . . .  | 14 | 5.10 Plotted residuals . . . . .   | 41 |
| 3.11 Galvanic isolation circuit for RS-232 . . . . .  | 16 | A.1 Schematic of reference voltages circuitry and ADC (single channel only) . . . . .  | 45 |
| 3.12 MicroSD card circuit . . . . .   | 17 | A.2 Schematic of MCU electrical circuit . . . . .  | 46 |
| 3.13 USB circuit . . . . .  | 17 | A.3 Schematic of circuits providing electrical power . . . . .   | 47 |
| 3.14 GPS circuit . . . . .  | 18 | A.4 Schematic of signal processing (single channel only) . . . . .   | 48 |
| 3.15 EEPROM circuitry . . . . .   | 19 | A.5 Schematic of RS-232 circuit . . . . .  | 49 |
| 3.16 Temperature measurement block of PCB and sensor head . . . . .   | 19 | A.6 Top layer of our PCB . . . . .   | 50 |
| 3.17 LEDs circuit . . . . .   | 21 | A.7 Bottom layer of our PCB . . . . .  | 51 |
| 3.18 Display circuit . . . . .  | 21 |  |    |
| 3.19 Rotational encoder circuit . . . . .   | 22 |  |    |
| 3.20 Used PCB enclosure (1455L1601 Hammond Manufacturing)[4] . . . . .                                      | 23 |  |    |
| 3.21 Detail of via stitching . . . . .  | 23 |  |    |
| 3.22 Block diagram of the PCB modules arrangement . . . . .   | 24 |  |    |
| 3.23 Visualization of produced PCB top layer . . . . .  | 25 |  |    |
| 3.24 Second layer of our PCB with ground planes and indicated direction of the excitation current . . . . . | 26 |  |    |
| 3.25 Third layer of our PCB with titled voltage planes . . . . .  | 26 |  |    |
| 4.1 Flowchart of device's start-up . . . . .  | 28 |  |    |
| 4.2 SPI interfaces diagram . . . . .  | 29 |  |    |



## Tables

|  |    |
|--|----|
| 2.1 Comparison with competition ...                                      | 5  |
| 4.1 EEPROM mapping .....   | 34 |
| 5.1 Scalar calibration output for X, Y,<br>Z channels respectively ..... | 42 |
| B.1 Control commands set .....   | 53 |



# Chapter 1

## Introduction and motivation

Fluxgate magnetometers are very interesting and delicate sensors. They are rather sensitive and have a high resolution meaning they find use in many practical branches including e.g. aviation, mapping Earth's magnetic field [6] or interestingly space physics [7, p. 217-225].

As of today, current market does not ultimately satisfy all needs for a fluxgate magnetometer with many optional features. This thesis aims to fill this gap by developing a fluxgate magnetometer with many attributes including a preferred choice of digital data output, whether it's saving, live transmitting or displaying.

Our product also includes such features as low noise signal processing, robustness, wide-range power supply voltage input, both stationary or mobile magnetic field monitoring, USB connection, MicroSD card output, RS232 communication, a GPS module, basic human-machine interface with OLED display and other.

Specifically, the goal was to construct such modular device with many extra features that are not usually seen on the market. Comparison of our product and commercially available products is also a part of this thesis.

Interestingly, we have been contacted with a request for a lightweight magnetometer capable of precisely measuring very small values of the magnetic field. This device would map anomalies in the magnetic field over Berringer Crater, Arizona. Although we are not developing exactly such a device, a very similar design would be viable for said purpose. This fact therefore makes up another part of overall motivation.



**Figure 1.1:** Berringer Crater, Arizona [1]



## Chapter 2

### Theoretical analysis

Before we address the development of our specific device, let us first make a small introduction to fluxgate magnetometers and magnetometers in general. As a part of this analysis, a comparison of our product with commercially available ones is included.

#### 2.1 Magnetometers

As Ripka states, magnetometer is a device that has two possible definitions. One of them measures the magnetic field and the second one the magnetic moment [2, p. xvii]. Fluxgate magnetometer is a part of the first group and anytime a magnetometer is mentioned in this thesis, the first definition is the desired one.

We may recognize magnetometers functionally based on various principles. Those would be, apart from fluxgate magnetometer, e.g. induction sensors, Hall-Effect magnetic sensors, Magnetoresistors, Superconducting Quantum Interference Devices (SQUIDs) [2, p. vi-xi] etc. There is also one critical specification and that is whether the magnetometer is scalar or vector.

The field of application varies based on magnetometer type. This may include space physics [8, p. 250][7, p. 217-225], geophysics [9], unexploded ordnance [10] or archaeology [11].

#### 2.2 Fluxgate magnetometer

Fluxgate magnetometers are used broadly as of today. They are utilized in, among other fields, space [8, p. 250][7, p. 217-225], aircraft and vehicle navigation [2, p. 75] and monitoring Earth's magnetic field [6].

Fluxgate magnetometer uses a ferromagnetic core with two windings. One is the excitation winding that by alternating current periodically saturates the core in both directions. As a result, the value of permeability drops and the flux is "gated". The other winding is a sense coil that picks up induced voltage. When external magnetic field in direction of measurement is present, the core gets more easily saturated in one direction and less in the other. This change is then proportional to external magnetic field [2, p. 75-77].

We use the fluxgate magnetometer with second harmonic detection, which is despite many tried modifications still one of the most widespread principles [2, p. 90].

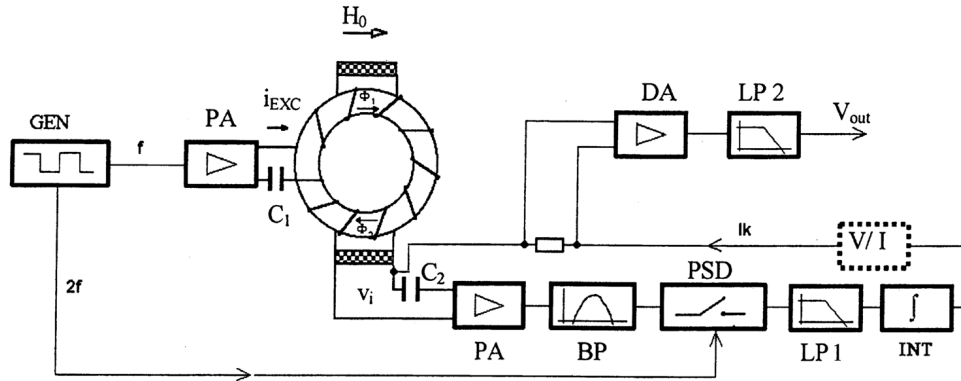


**Figure 2.1:** Block diagram of a second harmonic fluxgate magnetometer [2, p. 91]

We can see in figure 2.1 that the generator excites the sensor through an amplification and a capacitor that filters the DC component. As the sensor is excited, we receive signal on measuring coil. The second harmonic signal is preamplified and filtered in preferably RC bandpass. It is then processed through Phase Sensitive Detector (PSD) that ideally outputs a DC signal, which is then filtered through a low-pass filter. An integrator is added at the end for an amplification as the output is led to the measuring coil as a feedback signal through voltage-current converter. This converter may be as simple as a resistor. Current may then be measured on another precise sensing resistor as its voltage drop can be converted to digital data by an ADC [2, p. 90-93].

## 2.3 State of the art

If we look for commercial fluxgate magnetometers, we have to specify our demands first. Some of these basic requirements would be digital output, device mobility, furthermore measuring range, resolution, input voltage range, noise levels etc.

Knowing our device's specifications, we may arrive at a conclusion choosing the following three products available as of April 2018:

- DFM28G, by Billingsley Aerospace & Defense
- LEMI-029, by LEMI LLC.
- Mag658, by Bartington Instruments

If we refer to product data sheets [12][13][14], we may construct the following tables 2.1 comparing the basic features and specifications.

On a closer inspection we may see that our device offers one of the best resolutions, which is affected by the ADC choice. Measuring range we offer

|                                   | LEMI-029                        | DFM28G                           |
|-----------------------------------|---------------------------------|----------------------------------|
| ADC resolution [bit]              | 32                              | 28                               |
| Noise                             | 6 pT/ $\sqrt{\text{Hz}}$ @ 1 Hz | 3 pT/ $\sqrt{\text{Hz}}$ @ 1 Hz  |
| Measuring range [ $\mu\text{T}$ ] | $\pm 78$                        | $\pm 65$                         |
| Supply voltage [VDC]              | $\pm 5$ , +3.3                  | 16 ... 34                        |
| Output forms                      | RS-232, SPI                     | RS-232, RS-485                   |
| Sampling rate [Hz]                | 1, 10                           | 55, 125                          |
|                                   | Mag658                          | Our device                       |
| ADC resolution [bit]              | 24                              | 32                               |
| Noise                             | 10 nT RMS                       | 30 pT/ $\sqrt{\text{Hz}}$ @ 1 Hz |
| Measuring range [ $\mu\text{T}$ ] | $\pm 524$                       | $\pm 100$                        |
| Supply voltage [VDC]              | 10 ... 20                       | 6 ... 25                         |
| Output forms                      | RS-422                          | RS-232, USB, MicroSD             |
| Sampling rate [Hz]                | 50, 100                         | 500, 250, 62.5                   |

**Table 2.1:** Comparison with competition

is above-average. While the measuring range of our product is greater than that of other devices, quantization noise is kept low as well since the above-standard 32 bits ADC provides a high resolution. Also DFM28G has only a one ADC which means channels have to be scanned sequentially and there is necessarily some time delay between these samples. Overall noise values are negatively affected by the fact that we do not internally process data as we have aimed to reach a higher sampling rate. Our device indeed performs much higher in the aspect of the sampling ratio than other commercially available products.

The power supply voltage range of our device is also above-standard as it was one of the main aims of this project. Forms of output we have designed are more modern than commercial products' and are suitable for the need of mobility. Apart from standard RS-232 output, more possibilities are included. Mobility is preserved by the usage of a MicroSD card and a more practical and modern access is ensured by USB.





# Chapter 3

## Device conception

In this chapter we address the hardware related matters, i.e. the electrical circuit design and the PCB layout. Basic concept of the signal processing is based on that of a general fluxgate magnetometer as closer described in 2.2. We used open source EDA (Electronic design automation) software called KiCad for creating both electrical circuit design and PCB layout.

One of the main requirements for our device was mobility meaning that the PCB board with all the components would have to fit in a PCB enclosure, dimensions of which are suitable for portability. Other demands such as high resolution, low noise and extra features of course also highly influence components choice and overall design.

### 3.1 Electrical circuit design

Let us first describe arrangement of functional blocks using the figure 3.1.

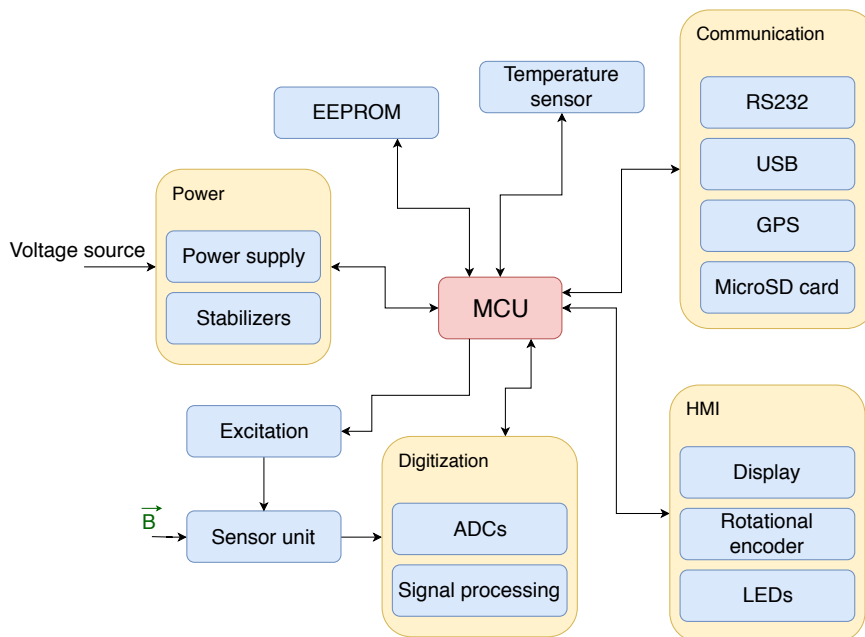


Figure 3.1: Block scheme of our fluxgate magnetometer

Looking at this block scheme, it may be seen that our device is digitally driven by MCU (microcontroller unit). While large portion of our design is digital (meaning data transfer is digitally encoded), analog parts are to be found here as well. This influences our conception since we use different ground planes that are however ultimately connected. More information on this matter is to be found in subsection 3.2. Each logical block will be further described in the following subsections.

### 3.1.1 MCU

Logical block of the microcontroller unit is one of the most critical ones in our design as every single module depends on it. The MCU we have chosen for our device is STM32L452VE, produced by STMicroelectronics.

This MCU runs on ARM® Cortex®-M4 32-bit RISC core implementing many above-standard features among which can be found: floating point unit, 512kB Flash memory, 160kB SRAM, 14-channel DMA controllers, Adaptive real-time memory accelerator, Memory protection unit [15] etc.

Among this MCU's other features we use are such as internal 12-bit ADCs, Real time clock (RTC), timers with PWM modes, multiple clock sources with phase locked loops (PLLs), General purpose input/output pins. There are also many communication interfaces prepared for our use: USB, USART, SPI and SDMMC [15].

Complete schematic of the electrical circuit can be found in the appendix A.2. MCU has multiple voltage inputs of 3.3 V, each of which is treated by blocking capacitors. We also use 3.3 V with filtered high-frequency noise using an inductor and a ferrite bead for the external analog power supply and positive reference voltage. Digital ground flag (GNDD) is utilized for the MCU's ground power supply (VSS), negative reference voltage and its peripherals.

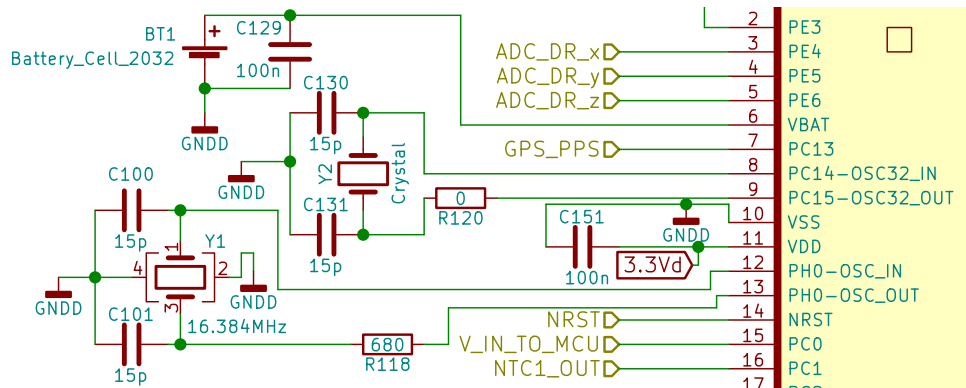


**Figure 3.2:** Circuitry of crystal oscillator and battery cell

We are using two external clock sources - crystal oscillators. We have chosen the frequency of 16.384 MHz for our high-speed external crystal (HSE) and we use 32.768 kHz for low-speed external (LSE) input. Using HSE is important as we need precise clock source for PWM timers as will be explained further

and clock choice rationale is e.g. that dividing the frequency will provide ADC with a sampling rate that results in the output of a whole number of samples per second. That is beneficial for further averaging and processing. Connecting LSE is suitable for our usage of real-time clock (RTC).

In order to use RTC independently of power source, we have included a connection to a battery cell that ensures functionality. Resistors of  $120\ \Omega$  value serve as elements that suppress signal reflection and reduce electromagnetic emissions by smoothing out edges. There is also a basic circuit for bootloader on pins 93 and 94. This is to be used in case of DFU (device firmware update) over USB. Using a general purpose output pin we may charge a capacitor, then if the device is restarted from firmware, the MCU will sense voltage on respective pin 94 (BOOT0) and will start in DFU mode.

Pins SWCLK, SWDIO and NRST connected to a jumper are used for programming MCU using the serial wire debugging (SWD) interface. Connection of programming pins is addressed in figure 3.3, which is added for completeness as it is excluded from any other functional blocks.

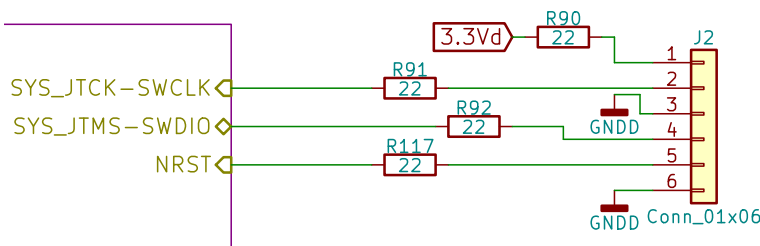


**Figure 3.3:** Connection of programming pins

Rest of pinout will be addressed further in respective subsections.

### ■ 3.1.2 Power

This crucial block ensures that all components of our device have their required respective voltage available. We shall divide this block into two sub-blocks, i.e. the power supply itself and regulators that adjust supply voltage for circuits.

Complete schematic of this block can be found in A.3.

#### ■ Power supply

The heart of this circuit is a DC/DC converter LTC3115-1. We supply this component with voltage range from 6 to 25 V. Once the device is running, it is possible for the input voltage to fall as low as 5.5 V. There are two possibilities of input. First is connecting directly onto jumpers with two wires between which is specified voltage. Second option is plugging in a DC power jack connector that is typical for 12 V adapters.

This circuit provides plenty of protection against harmful elements originated from power grid. In case of overvoltage we use both varistor and transil

in combination with 1 A fuse. These components will essentially short the circuit as current flows through them destroying the fuse but not damaging other parts.

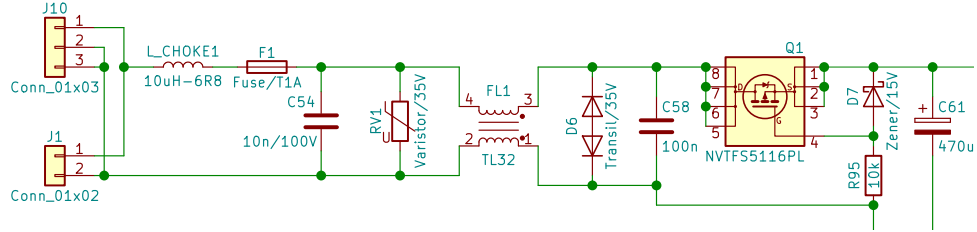


Figure 3.4: Protection on input of power supply

The design of the input also includes capacitors and inductors against spikes and sudden changes in the voltage level. There is also a circuit with a P-channel MOSFET that serves as a protection against reverse polarity. Then there is a bulk input and a bypass capacitor, as also suggested by application information of LTC3115-1 data sheet [16].

LTC3115-1 itself is connected mostly according to data sheet's typical applications section.

Output of this DC/DC converter is determined by a voltage divider, specifically given by the following formula 3.1 [16]. We have set it to 6 V.

$$V_{OUT} = 1 \left( 1 + \frac{R_{70}}{R_{71}} \right) V \quad (3.1)$$

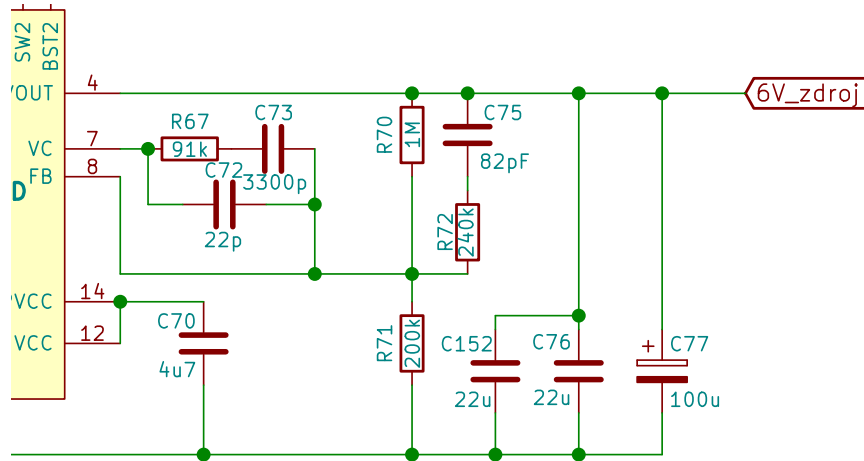


Figure 3.5: Output of LTC3115

Since the top resistor of the voltage divider determines quiescent current, choosing its value as 1 MΩ is acceptable [16]. That leaves the value of 200 kΩ for bottom resistor.

## Regulators

We utilize five linear regulators in this section for our device. All of their inputs are connected to 6 V from main power supply as described in the previous section.

- 3V3 regulator is very important as it provides voltage for a large portion of digital part of our design. This voltage is required by MCU, EEPROM, MicroSD card, GPS module etc. This integrated circuit (IC) needs no setting of output value as it is manufactured to provide 3.3 V.
- 2V5a regulator outputs necessary supply voltage for AD converters. This IC also doesn't need any output adjusting.
- 5V5a regulator is used for supplying circuitry concerning AD converters, specifically operational amplifiers and precision reference of 5 V, LTC6655. We set the output by choosing the resistor  $R_{53}$  by the following formula 3.2 [17].

$$V_{OUT} = R_{53} \cdot 1 \text{ mA} \quad (3.2)$$

- 5Va regulator is the main voltage source for the analog part of our design as it supplies operational amplifiers and triple SPDT switch. Output is set in the same manner as 5V5a case.
- 5V5exc regulator's sole purpose is providing the power for excitation of the fluxgate sensor. As large currents may flow through concerned circuitry, it was suitable to place an extra regulator into our design. It is also the preferred solution so as not to cause any interference in our sensitive analog part. We have set resistors as proposed in figure 3.6 to meet our needs [3]. Excitation voltage is also properly treated against sudden consumption changes by a large  $470 \mu F$  capacitor.

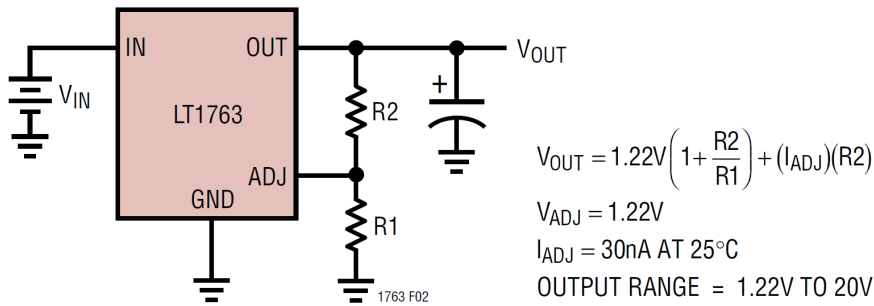


Figure 3.6: Adjustable regulator LT1763 [3]

### 3.1.3 Excitation

In order to excite the fluxgate sensor, we incorporated a driver unit with an H-bridge that consists of two double power MOSFETs (each with a one P-Channel and a one N-channel) and respective MOSFET drivers.

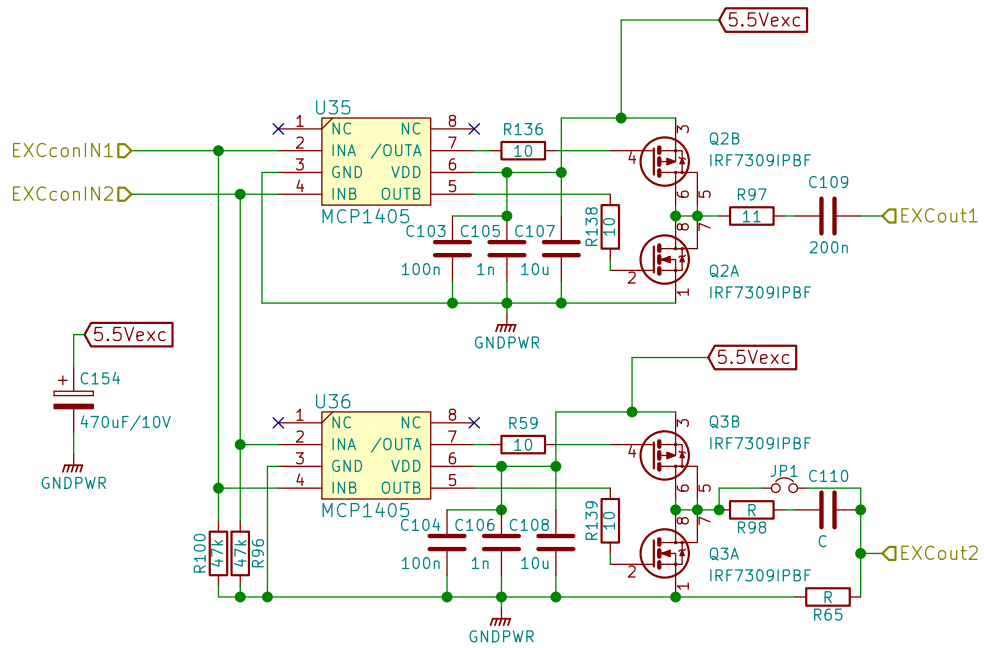


Figure 3.7: Excitation circuit

Supply voltage of drivers is properly stabilized by three capacitors. MOSFETs are connected to their respective drivers in accordance with data sheet [25]. Also input signals are normally tied to ground by pull-down resistors.

Gate of every single MOSFET has a resistor on input. This reduces current spikes and suppresses possible oscillations. Resistor and capacitor on the output of Q2 MOSFET set the amplitude and shape of the current excitation and filter the DC component as described in section 2.2. Their values were determined empirically. This procedure is described further in the chapter 5.

### 3.1.4 Digitization

After obtaining the signal from the sensor head, it needs to be processed suitably for consequent digital output that is further used by MCU. This part is once again in general done mostly in accordance with section 2.2.

### Signal processing

There are three output signals from sensor head, each signifying one component of a three-dimensional vector. Signal processing therefore comprises of three channels, each of which is identical to another. We will therefore address and describe a single channel only. Its complete schematic may be found in appendix A.4

Input signal's reference level is set to 2.5 V (2V5ref). Signal first flows through a common mode choke, eliminating noise. DC mode is filtered by an input capacitor and then the signal with reference level of 2.5 V is amplified by a non-inverting preamplifier. Double diode serves as protection that clamps

too high or too low voltage.

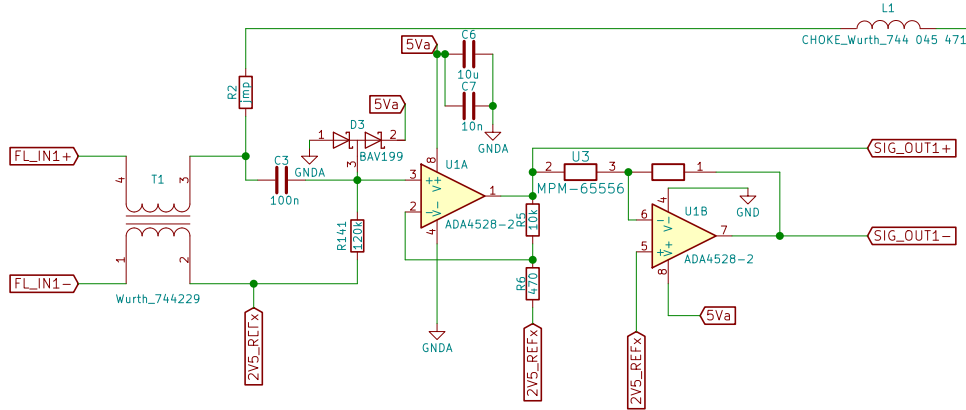


**Figure 3.8:** Input circuitry of signal processing

Gain of the operational amplifier  $U_{1A}$  can be calculated using the following formula.

$$A = \left(1 + \frac{R_5}{R_6}\right) \doteq 22.3 \quad (3.3)$$

The output signal is then inverted with the use of an inverting operational amplifier  $U_{1B}$  and a pair of precise resistors (two  $10\text{ k}\Omega$ ). Since the equation of the output signal is as follows, we should get nearly precisely inverted signal of input ( $R_i$  is input and  $R_f$  is feedback resistor of inverting operational amplifier).

$$A = -\left(\frac{R_f}{R_i}\right) = -\left(\frac{10\text{ k}\Omega}{10\text{ k}\Omega}\right) = -1 \quad (3.4)$$

Both inverted signal and its former version are then connected to a triple Single Pole Double Throw (SPDT) switch controlled by MCU which in combination with inverting amplifier replaces a PSD. Output of this component is then determined by the MCU's PWM signal with double the frequency of excitation's PWM voltage. Setting the phase of this signal essentially sets the phase of the sensor head's output. This task shall be described further in the chapter 5.

Output of the switch is then filtered using an inductor and a ferrite bead. Capacitor in series is currently shorted and reserved for future experimental use. Signal is then connected to the input of an integrator. A small resistor may be found at the output of the integrator, its purpose is to slightly lower the voltage as a precaution if the used operational amplifiers weren't with rail-to-rail operation and the measuring range of our device would consequently be reduced.

The voltage is then converted to a current on an extremely precise reference resistor, pins of which are indirectly connected to the ADC. Said current then, after being filtered by a choke, goes all the way back to a common mode choke on the output of the sensor head to close the loop so the sensor

operates as a zero indicator. Also the temperature drift of gain is reduced by increasing the ratio of resistors in feedback line to the resistance of measuring coil. Choosing a reference resistor with a low temperature drift is therefore vital.

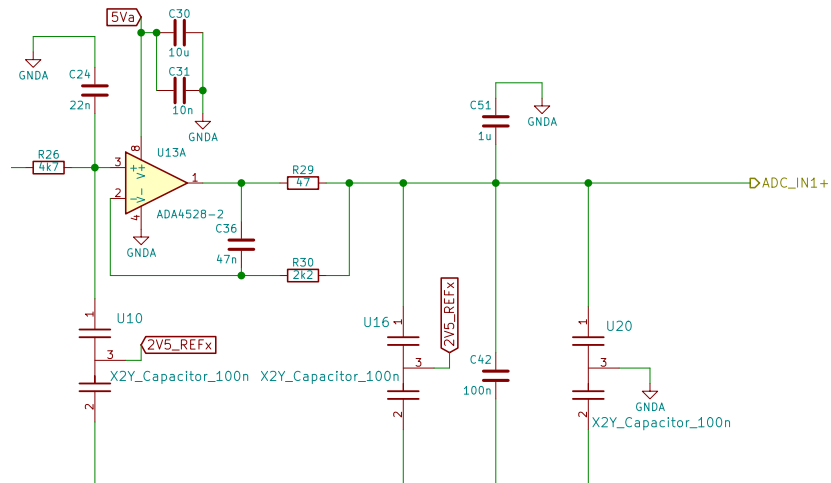


**Figure 3.9:** Unity gain buffer suitable for capacitive loads

Pins of reference resistor are then connected through resistors-current limiters to operational amplifiers that are essentially unity gain buffers (figure 3.9) suitable for capacitive loads as they suppress instability. Various kinds of capacitors are then presented in the design but their placement on the actual PCB is a matter of possible future testing.

### ADCs and reference voltage

In order to get good results from ADC, it is necessary to have a good reference voltage. We aim to achieve this by using LTC6655 IC, which is a highly accurate precision reference voltage source. Its output is 5 V and we use a simple voltage divider with ratio 1:1 to also obtain reference 2.5 V. Both input voltage and output voltage of the IC is stabilized by capacitors. Complete schematic of this block (single channel only) may be found in appendix A.1.

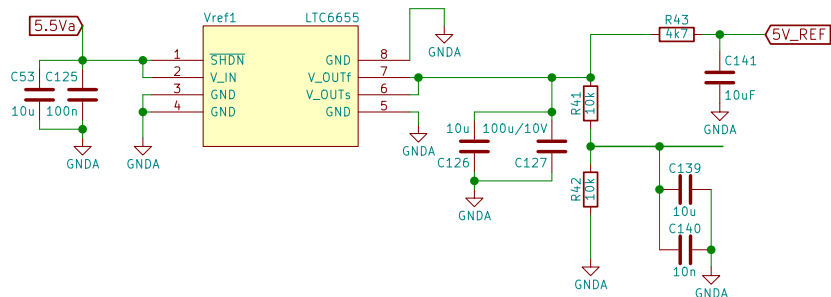


**Figure 3.10:** Reference voltage circuitry

Reference 5 V also pass through an RC integrator that has a function of



low band pass as such circuitry has positive impact on noise. This voltage is also buffered by a unity gain buffer for capacitive loads individually for each measuring channel. Reference 2.5 V level is treated similarly.

Used ADCs have 32-bit resolution, dynamic range of at least 131 dB and a low integral non-linearity  $\pm 0.5$  ppm. We also take advantage of their configurable integrated digital filter [26].

Connection is in a trivial manner. Power supply of 2.5 V, digital logic voltage of 3.3 V and reference voltage of 5 V are all connected with blocking capacitors tied to ground. Communication lines have resistors in series to eliminate the signal reflection. Master clock determines working frequency of ADCs, while Serial clock drives the pace of communication with MCU. On falling edge of DRL signal, data are ready to be retrieved through SDOA pin.

Pins SEL0 and SEL1 control the frequency of sampling and are adjustable on the run. SYNC pin serves for synchronization of simultaneous run of multiple ADCs, which we make good use of. RDLA pin has in practice a function of Chip Select that enables Serial Data Output A (SDOA) which provides filtered data. RDLB is pulled permanently to 3.3 V which disables SDOB that outputs 22-bit no latency code [26].

### ■ 3.1.5 Communication

The following section covers parts of our design that require communication with an externally connected device that may be used for data output, control or information retrieval (GPS).

RS-232 and USB serve both as means of controlling device and also as forms of measured data output. USB also has an extra feature of DFU as we will elaborate on later in this thesis in section 4.1.

Measured data may also be written to a MicroSD card, which is a feature ensuring mobility of our product.

GPS is used for the time synchronization and also possibly localization.

### ■ RS-232

We use one of the most widespread forms of sensor data outputs for our design - RS-232. Even though RS-232 goes a long way in the history of data transceiving and is no more a standard of newest electronic devices, it still finds use today because of its simplicity and functionality. Schematic of our entire RS-232 block may be found in appendix A.5.

RS232 circuitry requires ground and a power supply isolated from that of device. We have selected a centre-tapped power transformer with SN6505 transformer driver in order to achieve this task. SN6505 is connected accordingly to its data sheet [20] and its pin for enable signal is pulled-down when not activated by MCU. We have added an extra ferrite bead to filter high-frequency noise and extra capacitor that overall improves isolated voltage behaviour. Grounds on PCB are separated physically, as will be explained further in chapter 3.2. Capacitor  $C_{117}$  protects against possible voltage spikes between two separated circuits. This is vital to prevent the

ground loops in case of different ground potentials of the host and our device. Also (even indirect) lightning strikes could cause a voltage induction resulting in a possibly dangerous current.

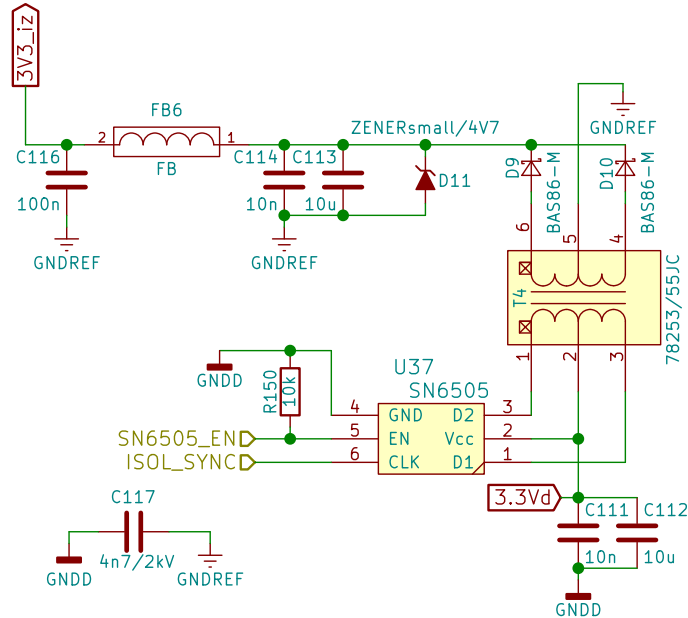


**Figure 3.11:** Galvanic isolation circuit for RS-232

Principle of work of the galvanic isolation circuit in figure 3.11 is that SN6505 serves as push-pull converter with open-drain pins. This means that always a one end of primary coil is tied to the ground while the second is disconnected. As the centre of the coil is attached to 3.3 V, this creates an alternating voltage, which is effectively transferred onto the second winding of transformer. This coil is then connected to diodes in a way to create a centre-tapped full-wave rectifier. The voltage is then smoothed out via capacitors.

Data signals are isolated by ADUM226N, a dual channel digital isolator. Signals are connected with resistors eliminating signal reflection. Power supply voltage inputs are treated by blocking capacitors. Voltage levels alone are converted to be RS-232 compatible by a well-known IC MAX3227E ( $\pm 25V$  input,  $\pm 5.4V$  output). Circuitry around this IC is connected in accordance with its data sheet, where external doubler-charge pump capacitors and inverting charge-pump capacitors are necessary [21].

Too high voltage on receive or transmit line is suppressed by Transient Voltage Suppression (TVS) diodes tied to the ground that protect against electrostatic discharge (ESD), electrical fast transient (EFT) and lightning [22]. Common mode noise is filtered by a common mode choke and  $47 \Omega$  resistors are used as current limiters if TVS diodes are activated.

## MicroSD

In order to keep our device mobile, we have decided to include a respective form of data output. Therefore it is possible only to plug in a MicroSD card, enable data logging for it and have the measured values saved there.

Circuit is once again straightforward - supply voltage is treated by blocking capacitors and all communication lines are connected to pull-up resistors. There are also resistors in series, mentioned in 3.1.1.

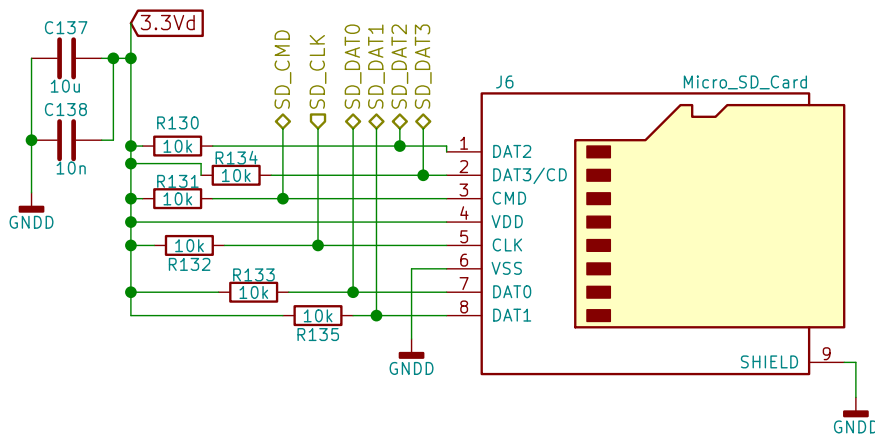


Figure 3.12: MicroSD card circuit

## USB

Since USB is lately a very popular choice for communication with every sort of digital device, we have included it in our design for control, data output and DFU. We have chosen mini USB connector for our purpose. Respective circuitry is not complex but some protection measures are applied, i.e. a fuse in combination with a TVS diode protect against ESD, EFT and lightning [23].

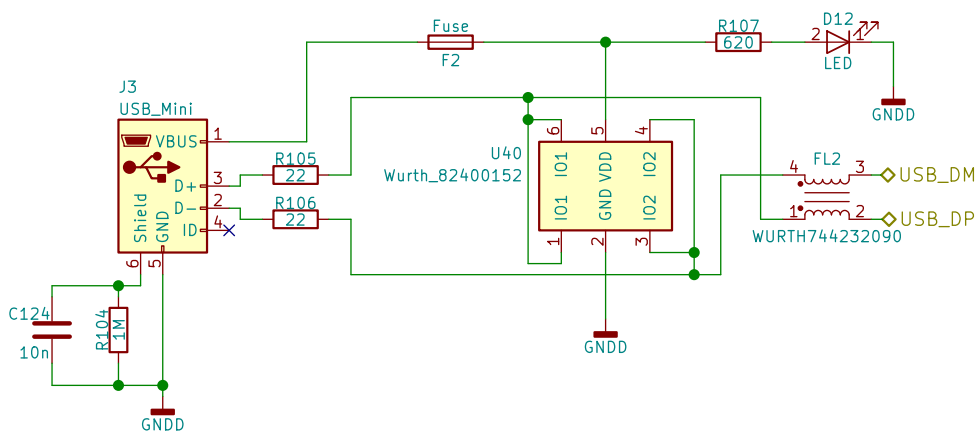
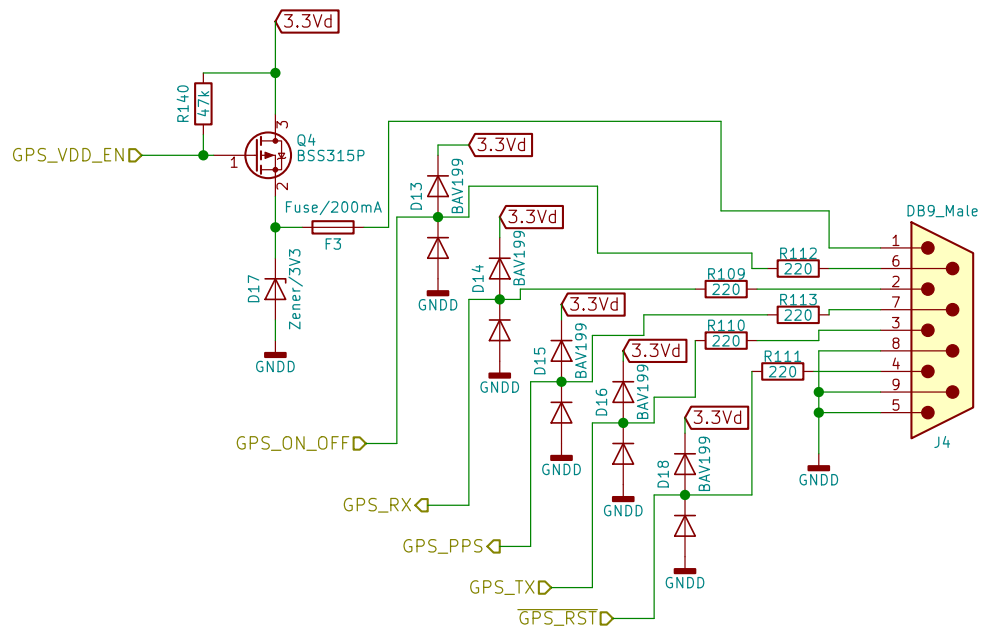


Figure 3.13: USB circuit

Signal LED lights up on USB connection just to inform that the USB has been plugged in. Common mode choke filters common mode noise in order to improve signal quality on D+ and D- data lines. Resistors in series on D+ and D- in our design were originally meant to match the characteristic impedance and possibly limit the current flowing into the TVS diode array although as we have learned on ST on-line forum, our MCU already has internal resistors to do the former. Shield of mini USB connector is tied to ground through RC filter in order to lower EMI.

## ■ GPS



**Figure 3.14:** GPS circuit

GPS is used for precise time synchronization and also localization using either GPS or GLONASS satellites. The external circuitry of ORG1518-R02 module designed by the supervisor of this thesis, Ing. Vojtěch Petrucha, Ph.D, is connected as a very simple USART interface with some controlling signals and a Pulse-Per-Second (PPS) signal.

We use resistors in series as current limiters and double diodes as a protection that clamps too high or too low voltage. In case the GPS receiver consumes too much power we use a P-Channel MOSFET as a switch for voltage. A Zener diode and a fuse are incorporated for a protection against high voltage or current.

### ■ 3.1.6 EEPROM

We have decided to use EEPROM (M95128, produced by STMicroelectronics) in our design as various user configuration may have to be saved throughout the lifespan of the device.

Although it would be possible to use MCU's internal Flash memory as an emulation of EEPROM, this solution is not suitable from the long-term point of view as the Flash memory may get corrupted much faster. It has been stated by ST that Flash memory of our MCU has a guaranteed minimum of 10 000 cycles endurance [18]. On the other hand, M95128 EEPROM has more than 4 million cycles and also a much greater data retention - more than 200 years as opposed to 7-30 years under various conditions [19].

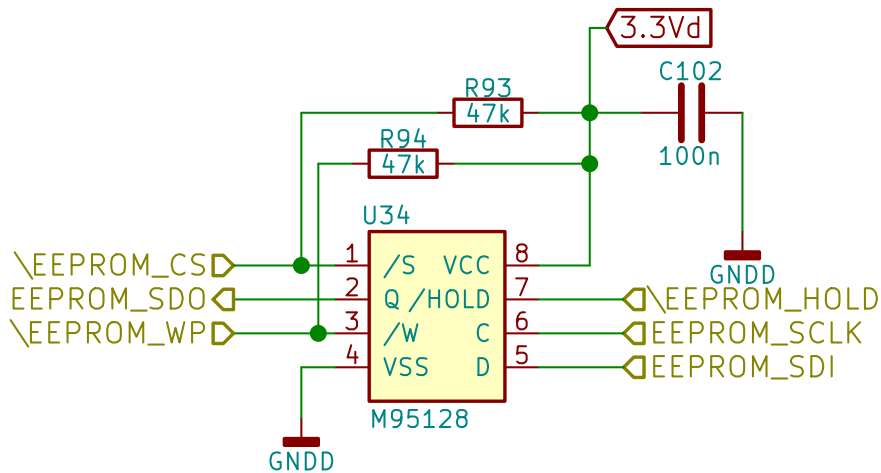


Figure 3.15: EEPROM circuitry

Circuitry as seen in figure 3.15 is rather straightforward as we use pull-up resistors for Write-Protect and Chip Select lines that are in a traditional manner active on low voltage level. Voltage input is treated by a blocking capacitor.

Our EEPROM's mode of work is SPI (Serial Peripheral Interface) which is in general faster than commonly used I<sup>2</sup>C (Inter-Integrated Circuit).

### 3.1.7 Temperature sensors

Two different temperature sensors are connected in our design. One of them is used for approximate monitoring of PCB temperature and the second one for measuring the temperature inside the external fluxgate sensor head.

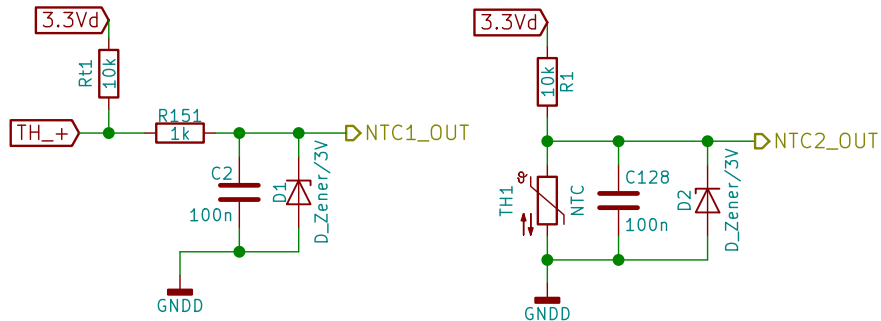


Figure 3.16: Temperature measurement block of PCB and sensor head



- Orange LED4 becomes active on UART/USB communication.

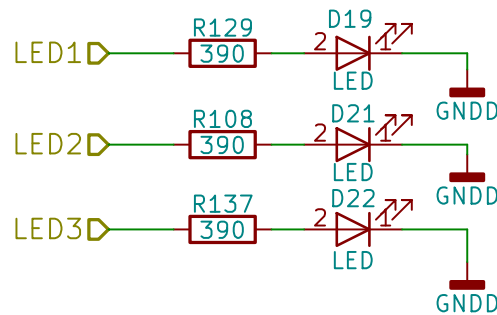


Figure 3.17: LEDs circuit

## Display

The display used for our application is Newhaven Display's yellow OLED type, 128x64 resolution with built-in SSD1325 controller [24].

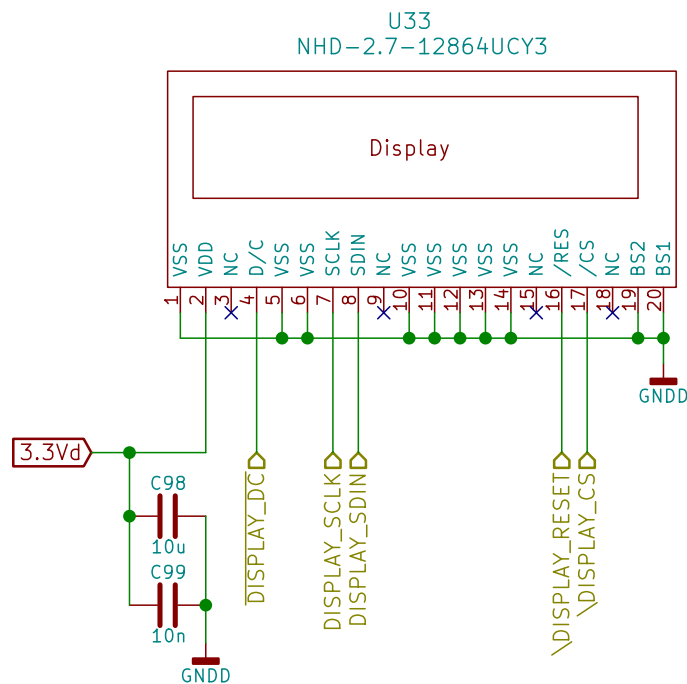


Figure 3.18: Display circuit

Since this display is already mounted to a small PCB, its interconnection with our design is rather simple - through jumper pins header.

Because our preferred choice of communication with the display is the serial interface (specifically Transmit only SPI), all that is needed are control, data signals and connected power supply. Tying BS1 and BS2 pins to ground specifies serial communication. This results in the connection of pins with accordance to data sheet where unused ones are tied to the ground [24].

## Rotational encoder

Direct control of the device can be assumed by using a rotational encoder with an included button.

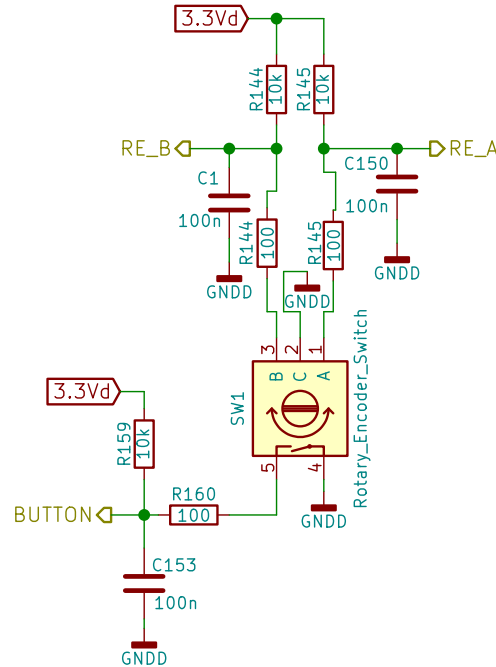


Figure 3.19: Rotational encoder circuit

Signals of rotational encoder are defined by the state of the encoder and pull-up resistors to 3.3 V. The output is treated by RC circuit where the capacitors debounce the signal and the resistors limit the current that would be caused by fast changes in voltage. Same circuitry is included for button.

## 3.2 PCB design

Since our device aims to be on state-of-the-art level, we have chosen a printed circuit board with four layers. Although they are more difficult to produce and much more expensive, they have a positive impact on reducing noise levels, EMI and the size of the board [27, p. 54]. As our device aims to be mobile, it has to fit into a hand-held sized enclosure that has milled openings for peripherals connectors. In order for the PCB to fit into our enclosure, dimensions of 162x98 mm have been chosen for the board.

Preferred choice of components was mostly Surface Mount Devices (SMD) although Through-Hole Technology (THT) was also utilized in special cases. This largely reduces the required size of the PCB. As our device is not primarily aimed for a serial mass production and we therefore solder all parts by hand, we did not follow the trend of downsizing [28][29] as we incorporate 0603 and 0805 chip types instead of smaller 0402 and 0201. Some parts of



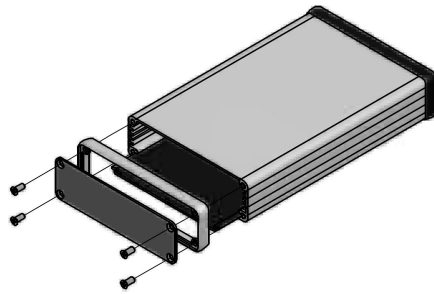


**Figure 3.20:** Used PCB enclosure (1455L1601 Hammond Manufacturing)[4]

our design also have power pads which aggravates hand-soldering as shall be described further in chapter 5.

Purpose of top layer of the PCB is primarily to connect individual parts through conductive tracks. In case a path for a track is difficult to find, it is possible to search for it in the bottom layer, which is the secondary layer for connecting components. Second layer then contains ground planes. Third layer from the top has multiple various voltage planes. Having two layers devoted only to power supply results in planes that benefit efficiency and stability [27, p. 54]. These areas effectively form a low impedance capacitor that reduces noise.

### ■ 3.2.1 General methodology

We have tried following principles described in [27] while designing PCB. Blocking capacitors are always placed as close to respective pin as possible. Power supply tracks are made very thick in case of expecting large currents in order to avoid power losses. Fast changing signals are on the other hand conducted through thinner tracks. Length of conductors, current loops and distance of crystal oscillator from MCU are overall minimized. We often connect a component to ground in more than one point.

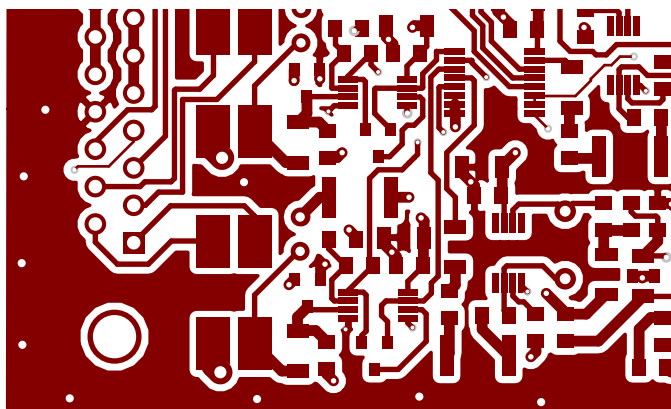


**Figure 3.21:** Detail of via stitching

We also use a technique called "via stitching", which vastly reduces EMI and can be seen in figure 3.21. It means that throughout the PCB's edges

many vias are added as they often sink emitted signals resulting in a better Electromagnetic compatibility (EMC) performance.

Parallel data signals are ordered by the expected pace of change (e.g. MicroSD data lines) as suggested by Záhlava [27, p. 52]. The total number of vias and tracks on bottom layer is decreased to as least as possible. On the other hand the placement of pull-up and pull-down resistors, imprecise voltage dividers etc. is often sidelined to make space available for more critical components.

### 3.2.2 Top layer

All components are mounted on the top layer and most of the tracks are located there too. Arrangement into functional blocks as seen in the figure 3.1 is mostly kept. Placement of the blocks can be seen in the following figure 3.22.

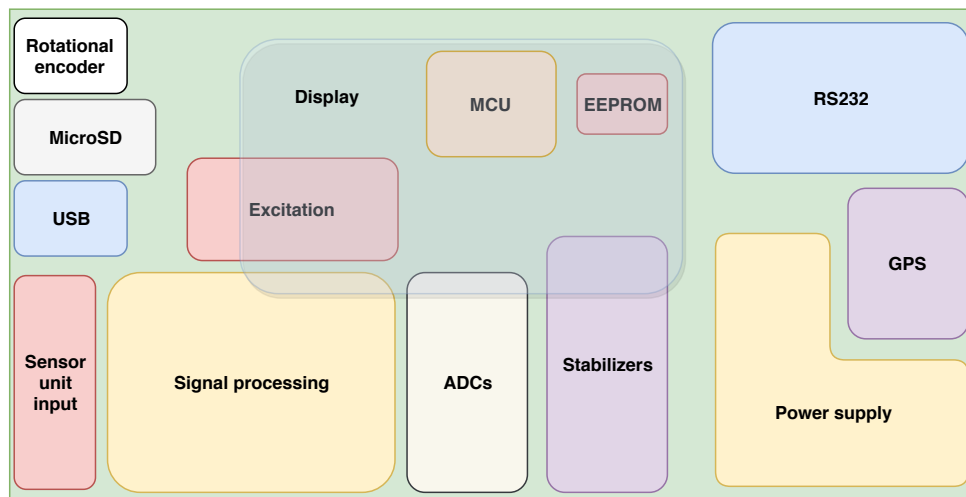


**Figure 3.22:** Block diagram of the PCB modules arrangement

Such placement is a careful configuration based on many factors. Block of sensor unit input, signal processing and ADCs are closely tied together in order to minimize picked up noise. Once the signal is digitized, readings become much more stable and we can allow the tracks to be longer as they lead towards MCU.

MCU itself is located roughly in the centre of design in order to be able to reach out to every block.

Power supply, GPS, RS232, Rotational encoder, MicroSD, USB and Sensor unit input block must all be located on the edge of PCB by nature in order to be accessible by user when the PCB is in the enclosure. Their specific location is then given by more factors - ergonomics, specific MCU pins accessibility. Stabilizers are placed close to the power supply as it is the first directly connected block.

Section of excitation (all the way from its respective voltage regulator) has its own reserved space as high currents are expected to flow, which could

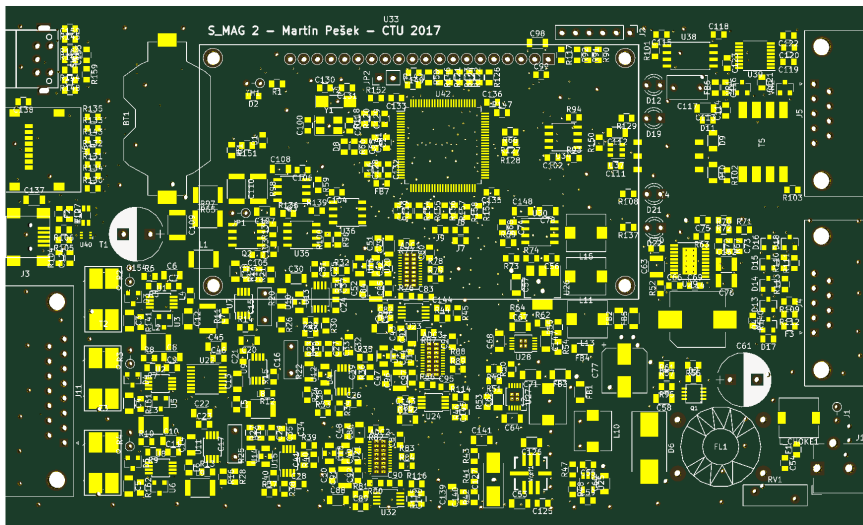


**Figure 3.23:** Visualization of produced PCB top layer

possibly interfere with other design parts, especially analogue one.

EEPROM is in the view of placement one of the less critical components and has been put close to its respective MCU pins. Display is positioned using a similar logic.

Rest of top layer is filled with the main ground plane with similar distribution to that of the second layer. It shall therefore be addressed in the following section.

### ■ 3.2.3 Ground planes layer

The second layer consists only of ground planes. Three grounds that are not interconnected may be seen but we could define up to five ground planes, three of which are however conductively joined. RS-232 and the power supply ground planes are isolated from the main one, which comprises of analog, digital and excitation ground.

RS-232 ground's isolation is necessary as described formerly in the subsection 3.1.5. Reference ground of external voltage supply is also isolated before it's filtered by a common mode choke.

Main ground plane has two non-conductive sections. Those were designed to separate analog ground. Its purpose is to hinder possibly large excitation current from interfering with sensitive analogue part of our design. Expected path of excitation current is indicated in figure 3.24. Digital ground would then be the rest of the main ground plane. Since the interference is not such a vast issue here, it is not separated from the excitation ground plane in any way.

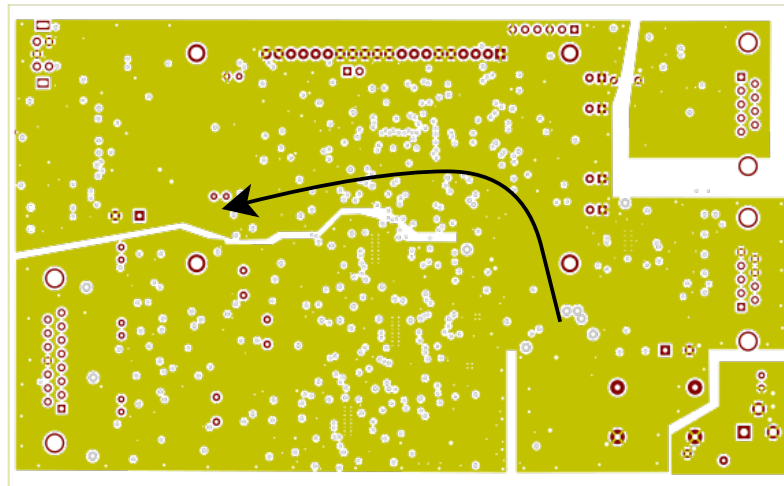


**Figure 3.24:** Second layer of our PCB with ground planes and indicated direction of the excitation current

### 3.2.4 Voltage planes layer

Because an entire PCB layer is dedicated to voltage planes, we tried to take advantage of it and fit as many various kinds of voltage in there as was viable. This is not entirely achievable because of various crossings in paths from pins to the respective voltage levels but we were successful to some extent. Planes are best to be viewed in figure 3.25.

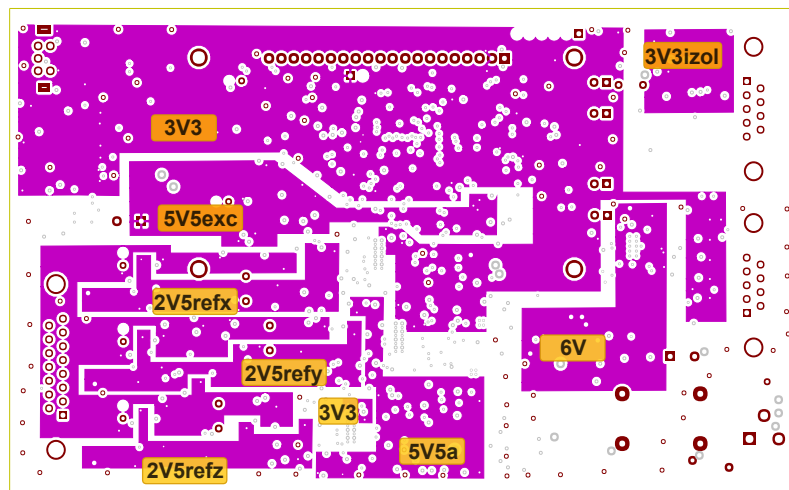


**Figure 3.25:** Third layer of our PCB with titled voltage planes

### 3.2.5 Bottom layer

Bottom layer is, as mentioned before, filled with tracks that we were unable to acceptably fit into the top layer. It is also filled with main reference ground.

Complete drawing may be seen in Appendix A.7.

## Chapter 4

### Firmware

In order to drive our device as desired, a solid firmware for MCU written in C programming language is required. It is necessary for this program to effectively interpret all sorts of user input - a rotational encoder, USB and RS-232. It also must be able to output data on any of these media - RS-232, USB and MicroSD card. All of these features must function independently as we wish to preserve the mobility and the universality. We have also included a feature of DFU when user unfamiliar with programming of ST microcontrollers may in few simple steps update the device. Our firmware has been in continuous development since July 2017.

#### 4.1 Basic concept

Our idea was to create a device that is capable of two kinds of operation modes. One is a single measurement when on command a single sample of values of three axes is made. The other one is a continuous measurement when data is being acquired without a break. User also has to be able to access some configuration of the device, specifically the data output options, date and time settings and the frequency of sampling. Other options like setting the phase of switching signal or configuring calibration constants are prohibited, as these are rather delicate matters that we had to perform with specific equipment and specialized methods. We have concluded that such settings therefore shall not be set from user-accessible menu.

The whole concept of our program is a state machine when actions are taken dependently on user input and previous state. We also have to take into account matters that happen "uncontrollably" such as DMA data transfers or interrupts services calling. There may be different ways of the program flow controlling but a state machine has shown to be very reliable. As time of development is limited and as the time factor has to be taken into consideration, way of the state machine proves to be a preferred one. Using available Real Time Operating System (RTOS) appears to be an overkill and unnecessary feature for our use.

Our code includes libraries provided by ST - specifically HAL and LL and external USB and FatFs libraries. Development has also been eased by the use of STM32CubeMX software. Copyright issues are dealt with directly in

code. Although usage of these modules critically facilitates programming, proper precautions have to be taken. As (especially HAL) libraries offer a great level of abstraction, resulting code is often less efficient and in extreme cases shows undesired behaviour as we will mention in the chapter 5.

## 4.2 Start-up

Upon plugging in power to the device, few simple routines are executed. This is best to be viewed in the following flowchart 4.1

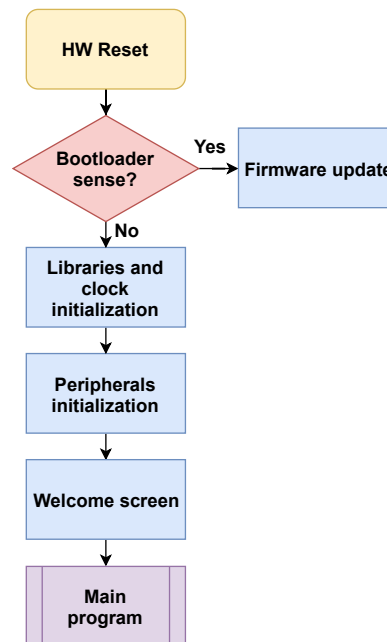


**Figure 4.1:** Flowchart of device's start-up

On the moment the device is turning on, if the MCU senses voltage on BOOT0 pin, bootloader stored in internal ROM starts up and the DFU mode is entered. If no voltage is present on BOOT0 pin, firmware from Flash memory is entered and our program starts to run. User may use dFuse application in order to load the new firmware to the device.

In such case, instruction, data cache and Flash memory prefetching are enabled firstly. Time base source is set to SysTick, inner timer of the processor core.

Clock settings are then initialized - clocks HSE, LSE, High-Speed Internal 48 MHz (HSI-48) are vital for the operation of firmware as rest of necessary clocks are derived from these by the means of prescalers. Implementing Phase-Locked Loops (PLLs) is indifferent for our design but they are set up from HAL libraries by default. Clock sources for peripherals are also set at this point.

After that, the GPIO groups are enabled and proper pins are initialized with the necessary configuration (output/input, inner pull-ups or pull-downs etc.).

This of course includes setting up pins with enabled interrupts - specifically two input pins for rotational encoder output and button input. Pins' default state is reset, which is beneficial because various IC are therefore not yet enabled and we can turn them on sequentially.

Since we have implemented the use of DMA, its controllers are initialized too along with the enabling of their interrupts. DMA critically improves the microcontroller performance as vast amounts of data do not have to be sent in blocking mode which saves a great lot of computing time. DMA has its downsides too as special precautions have to be taken - e.g. checking whether the data has been completely sent. Problems with DMA will further be addressed in chapter 5.

RTC is configured with desired settings like time format, no pin output etc. RTC should retain its values of time and date even after device reset as it is powered independently by battery cell.

Three SPI interfaces are introduced, one in "Transmit only master" mode, second in "Receive only master" mode. The former is used for sending data and instructions to the display and is configured for DMA as large data may be sent. The latter's purpose is obtaining the data from external ADCs. Third SPI, in "Transmit and receive full-duplex master" mode is needed for the communication with EEPROM.

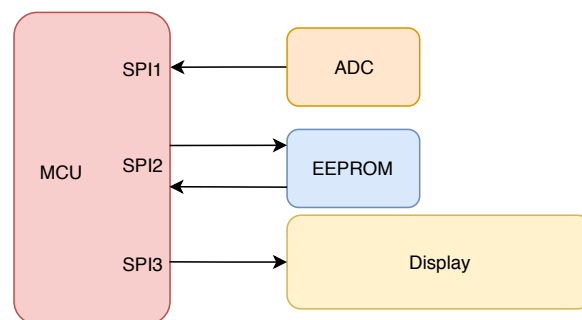


**Figure 4.2:** SPI interfaces diagram

USB peripheral is configured too, specifically in Communication Device Class (CDC) mode. This allows, provided that the user has the ST Virtual COM Port driver installed, to fully control our device over USB and receive data over it. USB is by default set to have interrupts enabled and send and receive data in non-blocking mode. USB has HSI-48 as its input clock.

Inner ADC is initialized as we utilize it for reading the PCB and the sensor temperatures and the input voltage. We need three channels for a single ADC meaning we find use in the Scan Conversion mode that allows us to read these three channels sequentially. We take advantage of built-in oversampling (16 times) feature [15] that gives us more precise [30] and stable readings. Since speed of conversion is not critical for us, sampling takes 640.5 ADC clock cycles. ADC is also configured to run in DMA mode in combination with an interrupt, which once again means a large upside as the program flow is not blocked.

Two UARTs are set up, one for GPS and the other for RS-232 communica-

tion (UART1). Baud rate for RS-232 is 115200 Bd/s and this UART is also configured in DMA mode. This is because sending measured data in blocking could severely affect the speed of samples reading. That would rapidly reduce the quality of our device.

We also initialize a timer that works on two channels with three outputs in total. First channel is set to Output compare mode with added negated signal and is used for H-bridge drivers signals with dead-time included. The second channel is in the PWM mode and is utilized for the triple SPDT switch (respectively PSD). Prescaler (PRE) of timer is set to 7, counter period (CP) to 79 timer ticks, and pulse (PLS) on channel 2 to 40 ticks. Since the channel 1 is set to toggle on a match with a value, it means that it outputs as same signal as on channel 2 but with half the frequency.

Expected frequency of the signal on the channel 2 can be calculated from HSE clock with 16.384 MHz frequency (respectively equivalent PCLK1) the following way:

$$f = \frac{PCLK1}{(PRE + 1) \cdot (CP + 1)} = 25.6 \text{ kHz} \quad (4.1)$$

Duty cycle ( $d$ ) is set to 50 % using this formula:

$$d = \frac{PLS}{CP + 1} = 50\% \quad (4.2)$$

One more timer is initialized to provide the master clock for the external ADC. Its frequency is set to 1.024 MHz using analogous calculations.

After this, DMA, input and UART1 interrupts are enabled.

In our non-generated section of the code we enable regulators of voltages, external ADCs and galvanic isolator driver for RS-232. Current state of one of the rotational encoders output is read in order for interrupt mechanisms of rotational encoder to work properly (described further in section 4.3.2). A quick common synchronization pulse for external ADCs is generated and then the timers are started. Receiving through DMA of UART1 is prepared, EEPROM is configured and data from it are loaded and applied to internal runtime variables. Then the device is ready to start functioning.

Using own functions to control the display, a logo of CTU is loaded and then a welcome message with date and time is displayed. Then display's content is erased and main program is entered.

## ■ 4.3 Main program

After start-up, the core of our firmware is being executed.

### ■ 4.3.1 Front-end

User interface constitutes of the main menu with three choices - Single, Continuous and Configuration. The same interface may be controlled by three means - a rotational encoder, USB or RS-232, always with the same



possible actions and the same result, except for the DFU request that is available via USB and RS-232 only. Providing such unified environment benefits not only a better user orientation in the device but also a cleaner and smaller code. In general the cursor on the display is moved in case of the encoder turning and an option is selected by pressing the button. Complete list of possible actions via RS-232 or USB may be found in the table B.1.

- Upon entering the Single mode, one measurement is made and displayed. User then has an option to either return to the main menu or to repeat the measurement.
- When the Continuous mode is selected, measuring is done without a break and values are refreshed on the display with a frequency of 10 Hz. User may either turn off display to lower the consumption and get faster data output rate or he may exit to the main menu.
- Last option to choose is the Configuration. This opens up another menu when one may change some basic settings. This includes toggling forms of data output - RS-232, USB and MicroSD card. Other options are changing the date and time and setting the ADC sampling rate, which directly influences data output rate.

The described interface is the best to be viewed in the following flowchart 4.3.

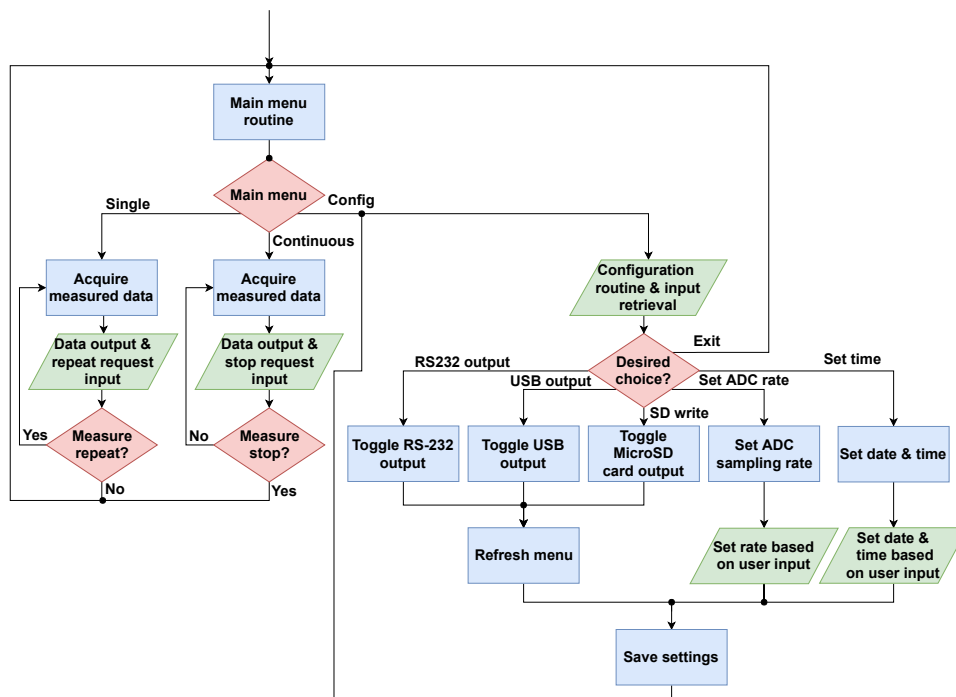


Figure 4.3: Flowchart of device's main program

### ■ 4.3.2 Back-end

Main part of our firmware is a state machine. Its states correspond with the list of user accessible modes and actions. We have therefore six states - Main menu, Single, Continuous, Configuration, Set time and Set rate.

At the end of every state machine iteration, the next state is assigned and if there are any requests from peripherals for a change of state then this request is acknowledged. Also by means of time-out mechanism, inner ADC is started for a conversion every half a second.

### ■ States

Every state has a similar service routine. There are actions taken based on reaching the state, the first entry of it, rotational encoder movement and the button pressing. Respective functions from separate modules are called during these routines.

On the first entry of a state, the screen is refreshed as new kind of graphical interface has to be shown. Respective strings of text and cursor signifying current choice are displayed.

Reaching the state in general causes only values that didn't retain their last state to change. This reduces the payload of unnecessary data transmitting with every refresh of screen. In case of continuous mode this means that we poll for new data from external ADCs and then once the data are available, we send them via the output peripherals or save them to a MicroSD card. If the user is located in the Main menu, the meta values of the temperatures and the input voltage are refreshed.

If movement of rotational encoder or press of a button are registered, display and miscellaneous functions are called in order to change the screen and the flow of the program.

### ■ Interrupts

We find use in a few interrupts. Most of them are the DMA callbacks that tell us a transfer is complete. This is used for both receiving and transmitting. Inner ADC, USB, RS-232, display and rotational encoder all make use of using interrupts. When data is received over RS-232 or USB, it is immediately copied into a global cyclical buffer. The rotational encoder and the button both have enabled interrupt on input pins. Respective routine then takes care of firmware debouncing and the signal interpreting. The ADC interrupt is called on complete conversion and we save the read values to our own buffer. Display's transfer complete callback is vital because we have to differentiate between sending the instructions and the data by setting the output pin `DIPSLAY_DC`.

## Modules

While many external libraries for our peripherals (e.g. display) already exist, we have decided to write some of the drivers ourselves as such method provides more control and ultimately better code efficiency. Let us now describe functions of these modules.

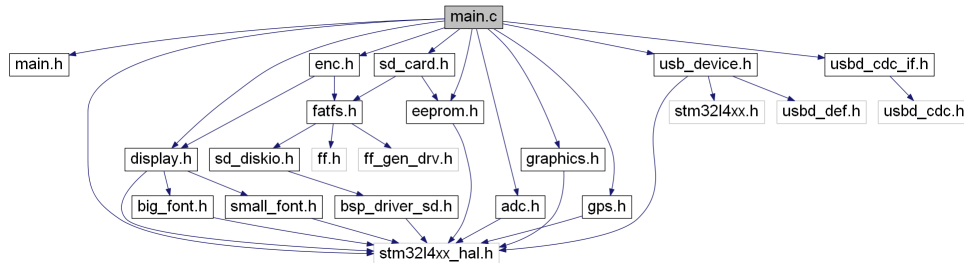


**Figure 4.4:** Basic modules dependency graph generated by Graphviz

- Main module contains miscellaneous system functions. That means some interrupt callbacks, output, calendar functions (like protection against inputting a bad date and time), higher layer menu and configuration functions are implemented here.
- Display module encapsulates service of display's SSD1325 driver. In cooperation with other modules, strings of text or even graphics may be sent. This module relies on DMA interrupt of transfer complete callback as previously mentioned. Functions providing the initialization and the refreshing of the display based on specific states are located here too.
- ADC module comprises of both lower and higher layer functions servicing external ADC. This includes retrieving read data and e.g. values calibration.
- Module of encoder includes functions that influence the control of the program flow. They are routines called when an action by user is registered.
- SD card module only provides a higher layer over included external FatFs libraries suitable for our firmware. We should note that below the layer of FatFs lies ST's BSP\_SD module that we had to rewrite as there seems to be an issue of cooperation with DMA. More information on this issue can be found in chapter 5.
- EEPROM module is a set of functions that communicate with EEPROM and load configuration directly into the runtime variables. Mapping of EEPROM as of now can be seen in table 4.1. Please note that the communication byte is an 8-bit number serving as a bit-map of enabled/disabled communication forms of output (RS-232, USB and MicroSD card).

| Data type          | Address (hex) | Data size (bytes) |
|--------------------|---------------|-------------------|
| ADC sampling rate  | 0x0000        | 1                 |
| Communication byte | 0x0002        | 1                 |

**Table 4.1:** EEPROM mapping

- Module of GPS provides the communication with the externally connected GPS receiver. We obtain a National Marine Electronics Association (NMEA) string that is further parsed. The specific data we are interested in are date and time, altitude, coordinates and number of satellites. Furthermore the PPS signal is also set up to increase the precision of RTC.
- The `big_font`, `small_font` and graphics modules are referenced by the display module. They are essentially only look-up tables of data to be sent to display using their proper respective functions. Tables of `big_font` and `small_font` are downloaded from an external source and are further referenced in the source code.

## Chapter 5

### Realization

The development of our fluxgate magnetometer has started in July 2017 when the supervisor of this thesis Ing. Vojtěch Petrucha, Ph.D prepared a development kit with a similar processor (respectively a Nucleo board) and some expected peripherals - a display, an SD card and an EEPROM. We have therefore been writing firmware modules for almost a year. Hardware development has been under way since September 2017 and was a much more problematic process as we have experienced some major setbacks.

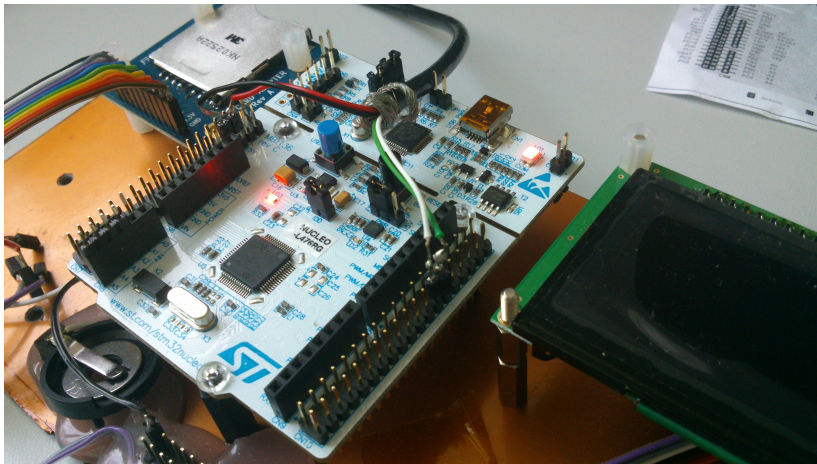


**Figure 5.1:** USB testing on our development kit

### 5.1 Firmware

We've had only a few drawbacks during the production of firmware. One of them was inappropriate setting of USB's clock. Formerly used MSI with PLL caused some instability during the enumeration phase of connecting to a USB host. Fortunately this issue was resolved by changing the clock to HSI48 as suggested on-line on ST forums.

The second major issue was the functionality of the MicroSD card writing and reading. ST's libraries have come out as insufficient in terms of functionality and DMA compatibility. This had to be resolved by rewriting parts of

libraries as one of DMA channels malfunctions. Solution to this problem was suggested on ST forums by ST staff.

## 5.2 Hardware

Matters were more problematic in case of hardware. Drawings of circuitry and the PCB might have been time consuming but the real issues appeared when the assembly and the testing of functional blocks started. During the soldering of components with power pads a heat gun had to be used and when one of the stabilizers was being mounted, we physically broke it. This resulted in a time setback as the same component had to be ordered again and further development was temporarily hindered.

We have soldered and tested out blocks individually which greatly helped to put the device to operation. However in order for better limitation of current, we have been running the device with 6 V connected directly to the output of DC/DC converter. Unfortunately as we have apparently used an inappropriate laboratory source of voltage, two regulators were destroyed - one in such a way that caused a short which damaged an operational amplifier on the Z channel. Even though a lot of time was lost once again, the shorted circuit fortunately hasn't affected other parts of the PCB.

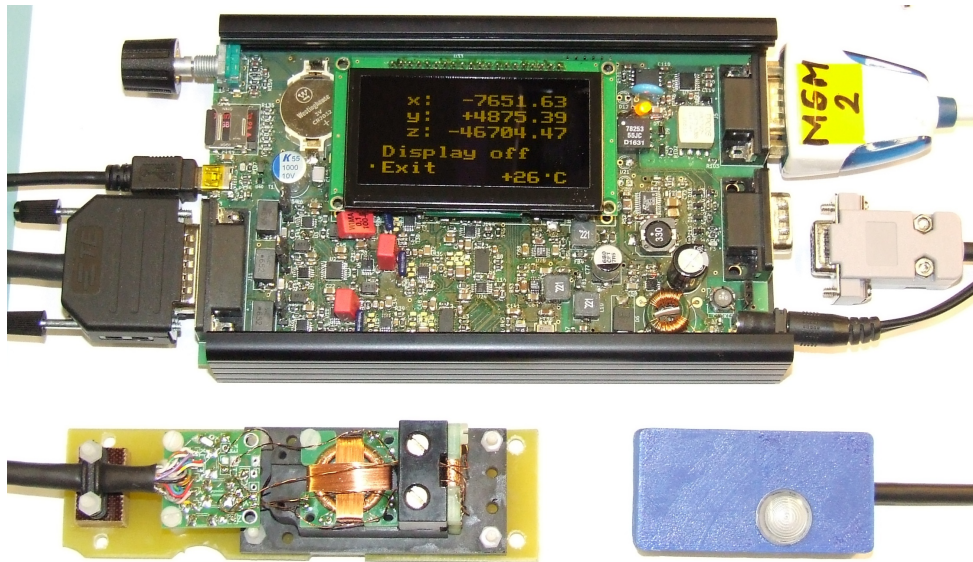


**Figure 5.2:** Finished and working device

Our device can be seen operating in figure 5.2. Continuous mode is set. There are also a fluxgate sensor head and a GPS receiver in the bottom part and both of these components were made by Ing. Vojtěch Petrucha, Ph.D.

## 5.3 Tuning

There were some parameters that we had to fine-tune after assembling the device. First was setting the resistor and the capacitor on the output of the excitation. Those were set to provide desired current and signal shape. Values we have empirically chosen as final are  $11\ \Omega$  for resistor  $R_{97}$  and  $200\ \text{nF}$  for capacitor  $C_{109}$ .

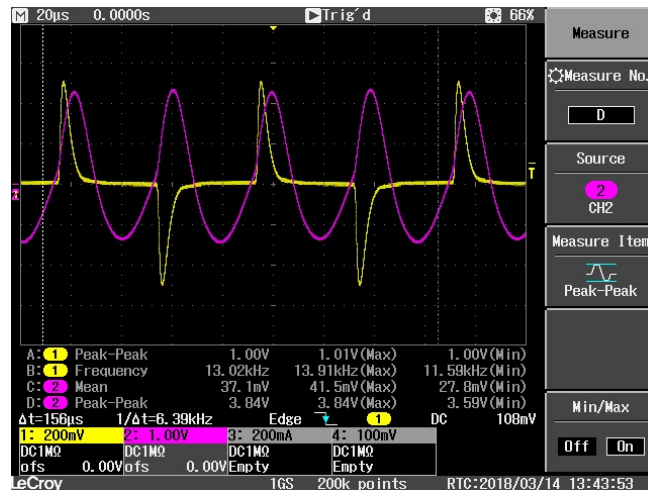


**Figure 5.3:** Tuning of the second harmonic on the sensor output (purple) and excitation current (yellow)

We've also had to set the phase of signal by setting the Capture Compare Register 1 of the timer. Since two sensors are in series, the third sensor is expected to have its output voltage a little shifted in time. Closer inspection however revealed that the best compromise is setting no phase as the desirable voltage curves are reached as closely as possible.

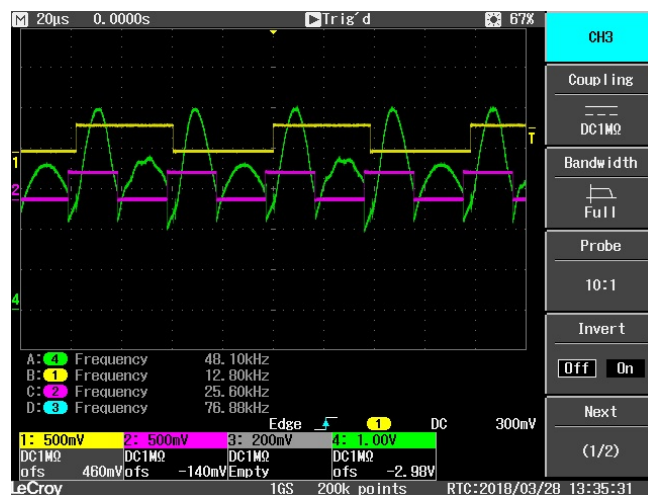


**Figure 5.4:** Setting the phase between excitation control voltage (yellow) and switching voltage (purple) by assessing the PSD output (green)

## 5.4 Parameters measuring

In order to get some specifications of our device, we have decided to obtain power spectral density as a measure of noise. Aim of this thesis was also to calibrate our device in order to get meaningful readings, i.e. convert the read digital number from ADC to an actual value of magnetic field (in nT).

### 5.4.1 Noise

Noise parameter was calculated by leaving the sensor head in magnetically shielded environment and taking samples for around five minutes. Using MATLAB we were then able to calculate Power Spectral Density. Please note that data were not averaged or filtered in software. The used script has been provided by Ing. Vojtěch Petrucha, Ph.D.

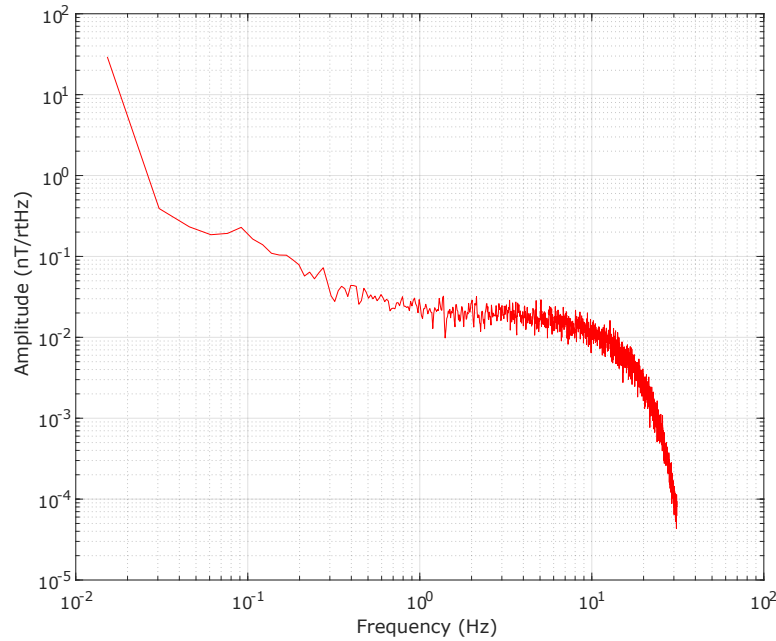


**Figure 5.5:** Noise spectral density of data sampled on Y channel with 62.5 sps sampling

### 5.4.2 Calibration

Device has undergone two kinds of calibration - vector calibration using 3-axis Helmholtz coil system and scalar calibration with a proton magnetometer. We consider our device a linear instrument, the function of which may be described in the following way as proposed and closer elaborated on in [5].

$$\mathbf{F} = \mathbf{S} \cdot \mathbf{P} \cdot \mathbf{B} + \mathbf{b} \quad (5.1)$$

$\mathbf{F}$  is the magnetometer output,  $\mathbf{S}$  the matrix of sensitivities (also referred to as "gain"),  $\mathbf{b}$  the offset vector and  $\mathbf{P}$  the matrix that transforms from the



orthogonal system to our imperfect non-orthogonal system.

$$\mathbf{F} = \begin{bmatrix} F_1 \\ F_2 \\ F_3 \end{bmatrix}, \mathbf{B} = \begin{bmatrix} B_1 \\ B_2 \\ B_3 \end{bmatrix}, \mathbf{b} = \begin{bmatrix} b_1 \\ b_2 \\ b_3 \end{bmatrix}, \mathbf{S} = \begin{bmatrix} S_1 & 0 & 0 \\ 0 & S_2 & 0 \\ 0 & 0 & S_3 \end{bmatrix} \quad (5.2)$$

$$\mathbf{P} = \begin{bmatrix} 1 & 0 & 0 \\ -\sin(u_1) & \cos(u_1) & 0 \\ \sin(u_2) & \sin(u_3) & \sqrt{(1 - \sin^2 u_2 - \sin^2 u_3)} \end{bmatrix} \quad (5.3)$$

Apart from matrix  $\mathbf{P}$ , all matrices comprise of relevant components of respective axes. Angles  $u_1, u_2, u_3$  are best defined in the following figure 5.6.

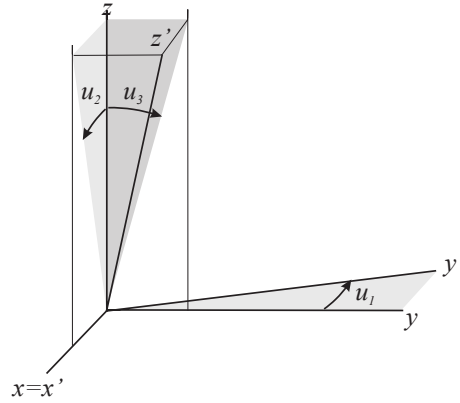


Figure 5.6: Angles defining non-orthogonality [5]

### ■ Calibration using Helmholtz coil

This calibration was the first one to be executed as its results were then to be made more precise by the means of scalar calibration. Also this method was relevant for us only in terms of determining the gain and offset of conversion functions. We have used MAGLAB group's equipment for this task.

Controlling system for Helmholtz coils provides the option of setting the magnitude and orientation of generated magnetic field via RS-232 interface. We have made three measurements activating always one axis only. This provides some independence and easier calculations.

We have measured for every channel from  $-100 \mu\text{T}$  to  $100 \mu\text{T}$  with the step of  $10 \mu\text{T}$ . This has also turned out to be approximately the range of our sensor. Let us now present one of the measured channel with a linear approximation of conversion function in figure 5.7.

Overall these functions seemed to be highly linear and with a low offset, which fluxgate magnetometers should have [2].

### ■ Scalar calibration

Scalar calibration requires a precise (proton precession) magnetometer in order to get the reference values of magnitudes of magnetic field. Based on

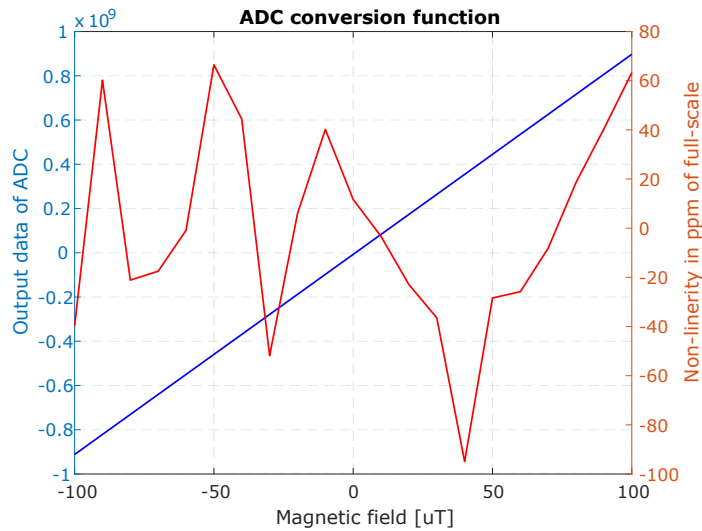


**Figure 5.7:** ADC conversion function for Y channel

the knowledge of our sensor head's rotation and the magnitude of magnetic field vector in more angle configurations, we are able to calculate individual components of the vector. This method, further described in [31], puts the linear least square method to use when iteratively estimating the calibration results.



**Figure 5.8:** Scalar calibration process in Průhonice

We have set out to Průhonice where less magnetic interference is expected to make these measurements. We have attached our sensor head to a turntable as also suggested in [31]. With every measurement, we have changed the configuration of angles on the turntable accordingly to a predefined set of 55 angles settings. Then we have always taken averaged samples from our device

and the reference proton magnetometer at the same time. The MATLAB script provided by Ing. Vojtěch Petrucha, Ph.D is then able to calculate the calibration constants based on the methods described in [31].

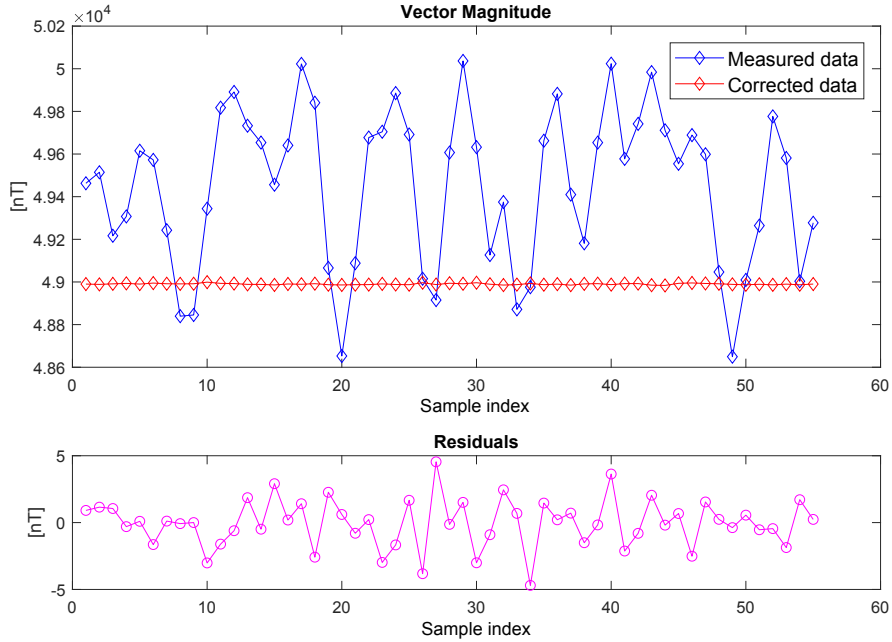


**Figure 5.9:** Scalar calibration plots of vector magnitude and residuals

Plot in the figure 5.9 shows correction of data, residuals (difference of measured scalar magnitude and the corrected computed vector magnitude). Figure 5.10 pictures plotted residuals in accordance with angles configuration during Průhonice measuring.

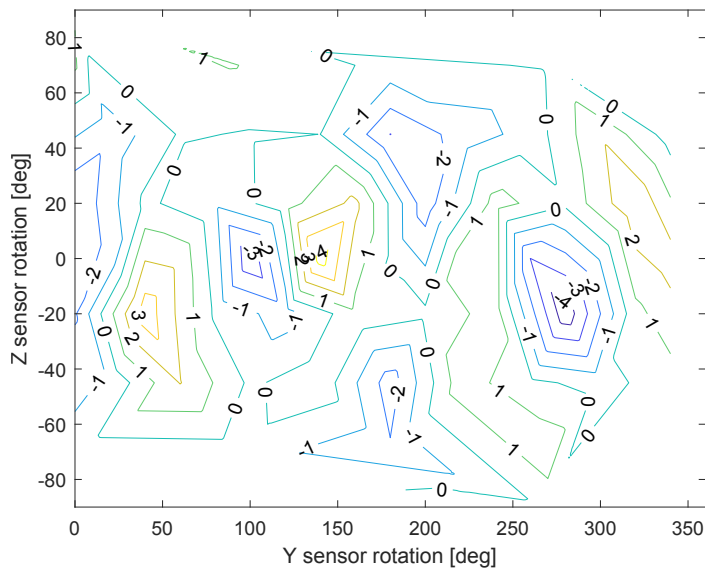


**Figure 5.10:** Plotted residuals

|                            |          |          |          |
|----------------------------|----------|----------|----------|
| <b>Offsets</b>             | -7.33    | -9.86    | -4.94    |
| <b>Scale values</b>        | 1.003293 | 1.009500 | 1.015426 |
| <b>Non-orthogon. [deg]</b> | -1.13378 | 1.00993  | -0.15103 |

**Table 5.1:** Scalar calibration output for X, Y, Z channels respectively

Results of these calculation are deemed satisfactory as gain values are very close to 1, meaning former vector calibration was successful. Offsets are also very low, which is a desired state. Some non-orthogonality is present but it is of no critical value. Calibration data as an output of provided script may be seen in the table 5.1.



## Chapter 6

### Conclusion

The aim of this thesis and the related project was constructing a universal digital fluxgate magnetometer capable of competing with today's state-of-the-art commercially available products in terms of not only the measurement quality but also the user interaction with the device including variable forms of data output. As concluded from 2.3 we have achieved better performance on many sides and it is therefore agreeable that our device proves to be viable for various kinds of measurements, e.g. mapping Earth's magnetic field. User has the option to operate the device in a stationary way or to keep the device mobile since the aim was to make a universal product. This means that there are more operational modes - one may only observe live measuring via display or output the data using a communication interface. This includes either connecting with a computer (via USB, RS-232) or just saving the measured values to MicroSD card. After some minor and major difficulties with both hardware and firmware, a successful outcome has been reached. The goal of this thesis was also to calibrate this device and compare it to commercially available products. We have performed this task successfully too.

Overall development of this magnetometer took almost a year and all the goals of this thesis were fulfilled but there are still ways to further deepen the development, e.g. creating a software with a graphical user interface that would let the user configure the device with ease. Perhaps further processing the measured data and incorporating them into a map by parsing the GPS module output would find its use with potential users. Also in order to create a more comfortable solution for some people, it would be possible to further filter and average the data. This of course effectively lowers the sampling rate of our device but ultimately improves noise performance. Some of these matters may be subject to change in the future as further testing should reveal needs for change.





# Appendix A

## Schematics drawings

**Figure A.1:** Schematic of reference voltages circuitry and ADC (single channel only)

**Figure A.2:** Schematic of MCTU electrical circuit





**Figure A.4:** Schematic of signal processing (single channel only)



**Figure A.6:** Top layer of our PCB





## Appendix B

### Control commands for terminal over RS-232 or USB

|                           |                               |
|---------------------------|-------------------------------|
| <b>Main menu</b>          |                               |
| s                         | Single measure                |
| c                         | Continuous measure            |
| r                         | Set configuration             |
| !                         | Restart device in DFU mode    |
| <b>Single measure</b>     |                               |
| s                         | Repeat measurement            |
| x                         | Exit to Main menu             |
| <b>Continuous measure</b> |                               |
| d                         | Toggle display                |
| x                         | Exit to Main menu             |
| <b>Configuration menu</b> |                               |
| r                         | Toggle RS-232 output          |
| u                         | Toggle USB output             |
| s                         | Mount or unmount MicroSD card |
| a                         | Set ADC sampling rate         |
| t                         | Set date and time             |
| x                         | Exit                          |

**Table B.1:** Control commands set





## Appendix C

### Bibliography

- [1] USGS and D. Roddy. 10. Meteor Crater, Arizona, United States. [https://www.lpi.usra.edu/publications/slidesets/craters/images/scraters\\_s10.jpg](https://www.lpi.usra.edu/publications/slidesets/craters/images/scraters_s10.jpg), 2002. [Online; accessed 4-April-2018].
- [2] Pavel Ripka. *Magnetic Sensors and Magnetometers*. Artech House, 2001.
- [3] LINEAR TECHNOLOGY. *LT1763 Series: 500mA, Low Noise, LDO Micropower Regulators*, 1999. Rev. H.
- [4] Hammond Manufacturing. *1455L1601*, 2014.
- [5] Nils Olsen, Lars Tøffner-Clausen, Torben Risbo, Peter Brauer, Jose Merayo, Fritz Primdahl, and Terry Sabaka. In-flight calibration methods used for the Ørsted mission. *ESA - SP on Calibration of Magnetometers*, 2000.
- [6] Lucas Pérez, David Ciudad, Marina Díaz-Michelena, and Claudio Aroca. Small fluxgate magnetometers: Development and future trends in Spain. *Sensors*, 10, March 2010.
- [7] Ayako Matsuoka, M. Shinohara, Y.-M Tanaka, A. Fujimoto, and K. Iguchi. Development of fluxgate magnetometers and applications to the space science missions, January 2013.
- [8] F. M. Neubauer et al. The Giotto magnetic-field investigation. *Space Sci. Rev.*, 23, 1988.
- [9] W. M. Telford, L. P. Geldart, and R. E. Sheriff. *Applied Geophysics*. Cambridge University Press, 1990.
- [10] H. H. Nelson and J. R. McDonald. Airborne magnetometry surveys for detection of unexploded ordnance. <https://pdfs.semanticscholar.org/fd2d/ef3b5034928b7a69cb2cfa92c43ddbcbfd5a.pdf>, 2006. [Online; accessed 1-May-2018].
- [11] F. Rainey. Archaeology: New tools for an old art: Thermoluminescence, magnetometers, satellite photography, and other techniques and instruments aid the archaeologist. *IEEE Spectrum*, 13, September 1976.

- [12] Billingsley Aerospace & Defense. *DFM28G 28 Bit Resolution Serial Digital Triaxial Fluxgate Magnetometer*, 2008.
- [13] LEMI LLC. *Digital Fluxgate Magnetometer LEMI-029*, 2016.
- [14] Bartington Instruments. *Mag658: Unpackaged Digital Three-Axis Fluxgate Magnetometer*, 2017.
- [15] STMicroelectronics. *STM32L452xx Datasheet*, May 2017. Rev. 3.
- [16] LINEAR TECHNOLOGY. *LTC3115-1: 40V, 2A Synchronous Buck-Boost DC/DC Converter*, 2012. Rev. B.
- [17] LINEAR TECHNOLOGY. *LTC6655: 0.25ppm Noise, Low Drift Precision References*, 2009. Rev. F.
- [18] STMicroelectronics. *STM32L4 - Flash: Embedded Flash memory*, 2017. Rev. 3.1.
- [19] STMicroelectronics. *M95128-W M95128-R M95128-DF: 128-Kbit serial SPI bus EEPROM with high-speed clock*, 2017. Rev. 19.
- [20] Texas Instruments. *SN6505 Low-Noise 1-A Transformer Drivers for Isolated Power Supplies*, 2016. Rev. September 2016.
- [21] Texas Instruments. *MAX3227E: 3-V TO 5.5-V SINGLE-CHANNEL RS-232 LINE DRIVER/RECEIVER WITH 15-kV IEC ESD PROTECTION*, 2006. Rev. June 2007.
- [22] Semtech. *SDC15: TVS Diode Array for ESD Protection of 12V Data and Power Lines*, 2004. Rev. 12/15/04.
- [23] Würth Elektronik. *Specification for release - Preliminary: 82400152*, 2010. Version 1.
- [24] Newhaven Display. *NHD-2.7-12864UCY3: Graphic OLED Display Module*, 2013. Rev. 2.
- [25] Microchip. *MCP1403/4/5: 4.5A Dual High-Speed Power MOSFET Drivers*, 2007. Rev. B.
- [26] LINEAR TECHNOLOGY. *LTC2508-32: 32-Bit Oversampling ADC with Configurable Digital Filter*, 2016. Rev. C.
- [27] Vít Záhlava. *Návrh a konstrukce desek plošných spojů*. Česká technika, 2005.
- [28] Brent Fischthal and Mike Cieslinski. Beyond 0402M placement: Process considerations for 03015M microchip mounting. [https://www.panasonicfa.com/sites/default/files/pdfs/Beyond0402Mplacement\\_ProcessConsiderationsfor03015M\\_Panasonic.pdf](https://www.panasonicfa.com/sites/default/files/pdfs/Beyond0402Mplacement_ProcessConsiderationsfor03015M_Panasonic.pdf), 2014. [Online; accessed 1-May-2018].

- [29] Michael Yuena, Heather Benedict, Kris Havlovitz, Tim Pitsch, and Andy C. Mackie. Tombstoning of 0402 and 0201 components: A study examining the effects of various process and design parameters on ultra-small passive devices. <http://citeseerx.ist.psu.edu/viewdoc/download?doi=10.1.1.594.655&rep=rep1&type=pdf>, 2014. [Online; accessed 1-May-2018].
- [30] E. N. Gilbert. Increased information rate by oversampling. *IEEE Transactions on Information Theory*, 39(6):1973–1976, Nov 1993.
- [31] J. M. G. Merayo, P. Brauer, F. Primdahl, J. R. Petersen, and O. V. Nielsen. Scalar calibration of vector magnetometers. *Meas. Sci. Technol.*, 11, 2000.